Radar visibility optimization under aerodynamic constraint for a wing profile

Francisco J. Baron Lopez

INRIA

INSTITUT NATIONAL DE RECHERCHE EN INFORMATIQUE ET EN AUTOMATIQUE

Radar Visibility Optimization Under Aerodynamic Constraint for a Wing Profile

Francisco Javier BARÓN LÓPEZ

N° 2073
Octobre 1993

PROGRAMME 6

Calcul scientifique,
modélisation et
logiciels numériques

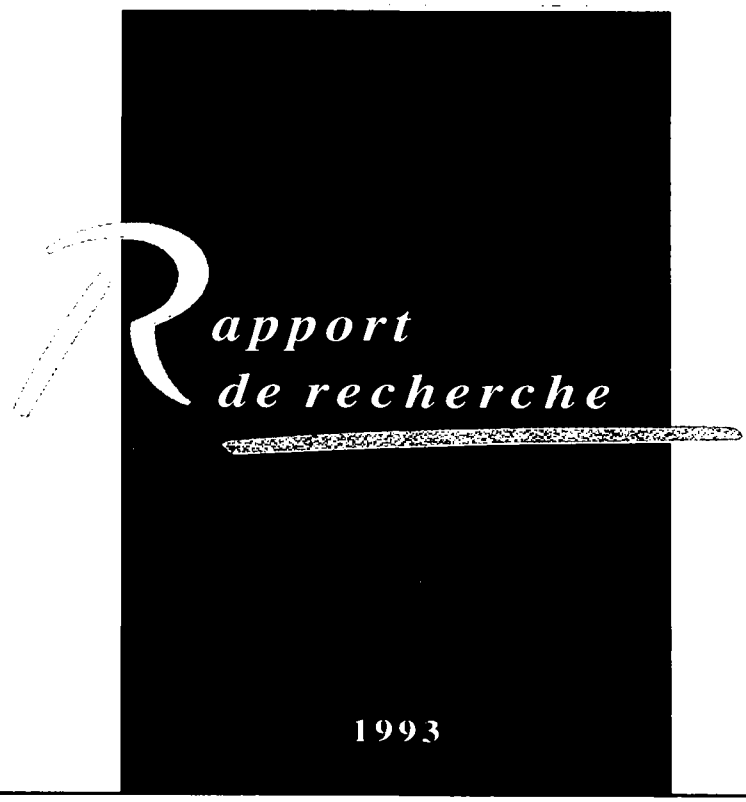

RADAR VISIBILITY OPTIMIZATION UNDER AERODYNAMIC CONSTRAINT FOR A WING PROFILE

Francisco Javier Barón López
Projet MENUSIN, INRIA, Rocquencourt
and
Dpto. de Análisis Matemático,
Facultad de Ciencias, Universidad de Málaga,
Campus Universitario de Teatinos s/n, 29080 Málaga, Spain.
e-mail: baron@menusin.inria.fr

RADAR VISIBILITY OPTIMIZATION UNDER AERODYNAMIC CONSTRAINT FOR A WING PROFILE

Francisco Javier Barón López
Projet MENUSIN, INRIA, Rocquencourt
and
Dpto. de Análisis Matemático,
Facultad de Ciencias, Universidad de Málaga,
Campus Universitario de Teatinos s/n, 29080 Málaga, Spain.
e-mail: baron@menusin.inria.fr

Abstract

We consider here the optimum design of a wing profile, with respect to aerodynamical and electromagnetical criteria and constraints. In these optimization design problems we have to face constraints of a very different nature (such as electromagnetic, aerodynamic, geometric,...). A new approach algorithm given by Herskovits has allowed us to solve succesfully the problem of finding a wing profile with minimum radar cross section under aerodynamic constraints on lift.

OPTIMISATION DE LA FORME D'UN PROFIL D'AILE POUR LA VISIBILITE RADAR SOUS CONTRAINTE AERODYNAMIQUE

Résumé

On considère ici le problème d'optimisation de forme d'un profil d'aile d'avion, pour minimiser sa visibilité radar, tout en satisfaisant certaines contraintes aerodynamiques et géometriques. Les variables d'optimisation sont la forme du profil d'aile et l'épaisseur de la peinture absorbante. Les contraintes sont géometriques (rayon de courbure par exemple) et aérody-

namiques sur la portance en approximation potentielle.

Keywords

Shape Optimization, Optimum Design, Finite Elements, Electromagnetics, Coating Paint, Fluid Mechanics, Aerodynamical Constraints, Partial Differential Equations, Nonlinear Optimization.

Contents

1 Introduction

We consider here the optimum design of a wing profile with respect to criteria and constraints of very different nature such as geometric, electromagnetic and aerodynamic. Our purpose is a methodology to reduce the radar visibility of a wing profile. The **constraints on the geometry** concerns the maximum and minimum thickness, radious of curvature; the **aerodynamic constraints** act on the lift, drag, skin pressure, ...

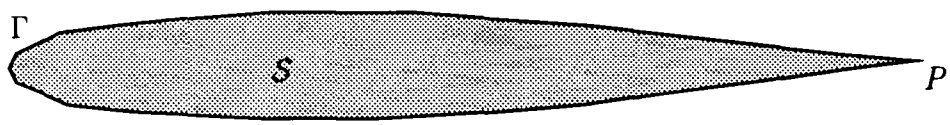

Figure 1.1: The wing profile

1.1 Optimum design problems

We shall use for our optimum design problem the notation of optimal control theory. The *control* is a curve $\Gamma = \partial\mathcal{S}$ in $\Re^2$: $\mathcal{S}$ represents a plane airfoil in dimension two. $\mathcal{S}$ belongs to a family of admisible designs $\mathcal{S}_{ad}$. $\mathcal{S}_{ad}$ includes the design constraints on $\mathcal{S}$. The wing profile Γ is the border of $\mathcal{S}$.

The *state* of the system $y_{\mathcal{S}}$ is solution of a partial differential equation written on the exterior of $\mathcal{S}$. Here $y_{\mathcal{S}}$ is the solution of Helmholtz' equation in $\Re^2 - \mathcal{S}$.

1.1.1 The cost function

We call it $j(\mathcal{S})$ and it depends on $\mathcal{S}$ also via $y_{\mathcal{S}}$:

$$\begin{aligned} j : \mathcal{S}_{ad} &\longrightarrow \Re \\ \mathcal{S} &\longmapsto j(\mathcal{S}) = J(\mathcal{S}, y_{\mathcal{S}}). \end{aligned}$$

Here it will represent the radar visibility of $\mathcal{S}$ with respect to the amplitude $y_{\mathcal{S}}$ of the wave.

1.1.2 The constraints

We consider on $\mathcal{S}$ two types of contraints: *geometrical* and *aerodynamical.*

The geometrical constraints: They are for example:

- $\mathcal{S}$ has only one connected component.
- $\mathcal{S}_1 \subset \mathcal{S} \subset \mathcal{S}_2$, with $\mathcal{S}_1$, $\mathcal{S}_2$ being fixed.
- Fixed length of the wing profile.
- Fixed angle at the trailing edge P.
- The changes of curvature are not large.

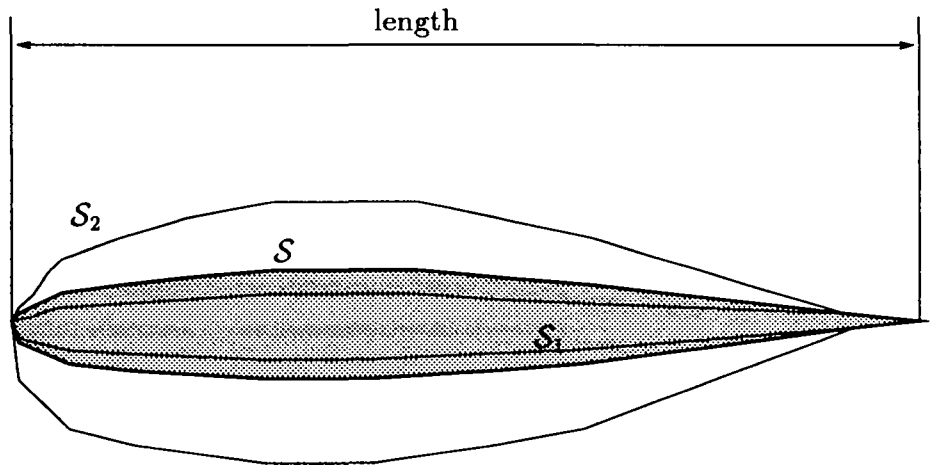

Figure 1.2: The geometrical constraints

The aerodynamical constraints: They would be for example:

- Let $\Lambda(\mathcal{S})$ be the lift coefficient of the wing for a fixed angle of incidence α. We can consider a constraint of the type $\Lambda(\mathcal{S}) > constant$.
- Constraints on the pressure field on Γ to prevent boundary layer separation.

The geometrical constraints are easily considered and described. Aerodynamical constraints are much harder because the dependence on the control $\mathcal{S}$ is given by Partial differential equations of fluid mechanics.
Here we consider only one aerodynamical constraint on the *lift* to be computed through a potential flow approximation. See [14][15][17] for the computations of some aerodynamical magnitudes that can be used as constraints in the optimum design problem.

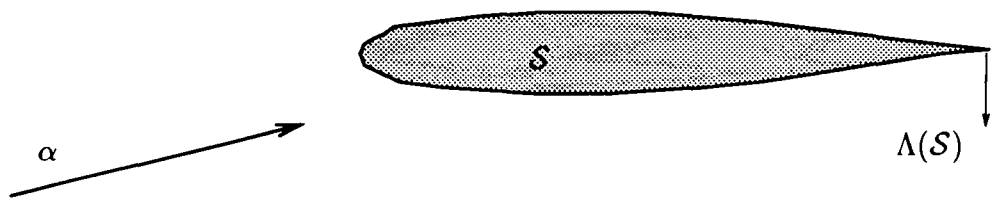

Figure 1.3: The lift

For the optimization algorithm with contraints we have chosen an algorithm due to *Herskovits* because it is robust and efficient. It generates a sequence of feasible designs with decreasing values of the cost. It is very important in optimum design problems that the sequence of *all* iterates be feasible.

1.2 Open problems

In control problems for optimum design we are interested to obtain the following results:

i) Existence of optimal domain.

ii) Characterization of optimum.

iii) Numerical approximation of the solution.

For **i)** and **ii)** it is necessary to know the derivative of a function

$$\begin{aligned} j : \mathcal{S}_{ad} &\longrightarrow \Re \\ \mathcal{S} &\longmapsto j(\mathcal{S}). \end{aligned}$$

But we have no vector space structure on the family of feasible designs $\mathcal{S}_{ad}$, so we must:

- Give a sense to the expression "$\mathcal{S} \longmapsto j(\mathcal{S})$ differentiable".
- Prove the existence of a derivative $j'(\mathcal{S})$.
- Compute an useful expression for $j'(\mathcal{S})$.

The computation of $j'(\mathcal{S})$ can be also useful for the numerical approximation, because it gives information of how to decrease the cost by modifying $\mathcal{S}$.

2 The continuous wave problem

2.1 The state equation

The scattering of the 2D plane stationary wave $z(\vec{x}) = e^{i\vec{k}\cdot\vec{x}}$ by an obstacle $\mathcal{S}$ in a homogeneous medium is described by the Helmholtz equation with the Sommerfeld radiation condition at infinity.

$$\begin{cases} \Delta y_{\mathcal{S}} + k^2 y_{\mathcal{S}} = 0 & \text{in } \Re^2 - \mathcal{S} \\ y_{\mathcal{S}} = z & \text{on } \Gamma \\ \lim_{r\to\infty} r^{1/2}\left(\dfrac{\partial y_{\mathcal{S}}}{\partial r} - i\,k\,y_{\mathcal{S}}\right) = 0. \end{cases} \tag{2.1}$$

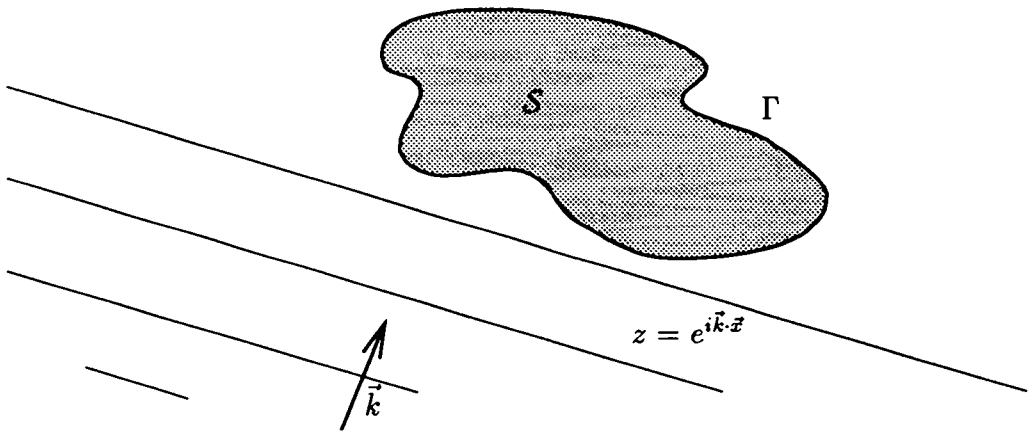

Figure 2.1: The incident wave

Here $\vec{x} = (x, y)$ is a point of $\Re^2$, $r = |\vec{x}|$, $\vec{k} = (k\cos\alpha, k\sin\alpha)$ is a wavevector of the incident wave z, where α is a an angle of incidence, and the complex valued function $y_{\mathcal{S}} = y_{\mathcal{S}}(\vec{x})$ is the diffracted wave.
We can use for $y_{\mathcal{S}}$ the following equivalent form of the Sommerfeld condition [5]:

$$\lim_{r\longrightarrow\infty} \sqrt{r} e^{-ikr} y_{\mathcal{S}}(r,\theta) = A(\theta). \tag{2.2}$$

The term $A(\theta)$ is the radiation diagram of the obstacle $\mathcal{S}$, i.e. the radiated power at infinity.
Another form of the Sommerfeld condition allows us to work with bounded domains. It consists in the introduction of a disk D of center 0 and radius R large enough in order to have

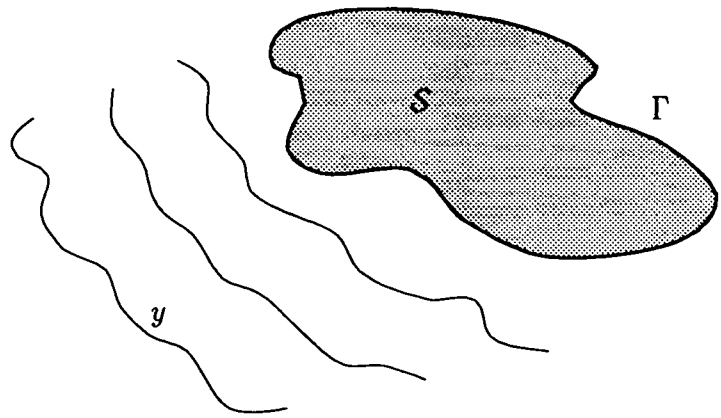

Figure 2.2: The diffracted wave

$$\mathcal{S} \subset D, \ \forall \mathcal{S} \in \mathcal{S}_{ad}. \tag{2.3}$$

Then the computational domain associated to the wing profile $\partial\mathcal{S}$ is $\Omega = D - \mathcal{S}$. We denote the family of feasible computational domains as:

$$\Omega_{ad} = \{\Omega = D - \mathcal{S} \ : \ \mathcal{S} \in \mathcal{S}_{ad}\}. \tag{2.4}$$

Let $\partial\Omega$ be the border of Ω. It is made of the wall of the wing $\partial\mathcal{S}$ and of the boundary of the disk:

$$\partial\Omega = \partial\mathcal{S} \cup \partial D = \Gamma \cup \partial D. \tag{2.5}$$

The way to obtain a boundary condition on ∂D equivalent to the Sommerfeld one, is the following. We suppose that the value $y(R,\theta)$ of the wave on ∂D is known. In that case the solution of the problem:

$$\left\{ \begin{array}{rcll} \Delta y + k^2 y & = & 0 & \text{out of D} \\ y & = & y(R,\theta) & \theta \in [0, 2\pi] \\ \lim_{r\to\infty} r^{1/2}\left(\dfrac{\partial y}{\partial r} - i\,k\,y\right) & = & 0 & \end{array} \right. \tag{2.6}$$

is (see [18] for example) of the form:

$$y(r,\theta) = -\sum_{n=0}^{\infty}{}' \frac{1}{\pi} \frac{H_n^{(1)}(kr)}{H_n^{(1)}(kR)} \int_0^{2\pi} \cos n(\theta - \theta')\, y(R,\theta')\, d\theta', \tag{2.7}$$

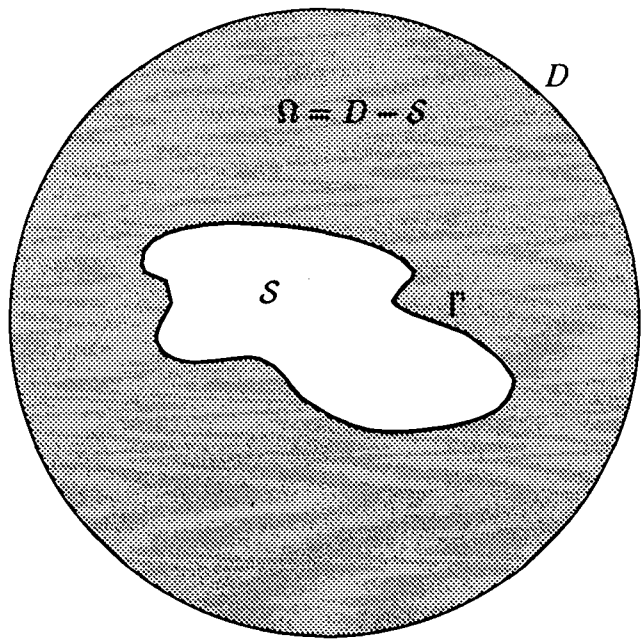

Figure 2.3: The computation domain

where $H_n^{(1)}$ are Hankel's functions of first kind, with the convention that

$$\sum_{n=0}^{\infty}{}' a_n = \frac{a_0}{2} + \sum_{n=1}^{\infty} a_n. \tag{2.8}$$

Differentiating with respect to r, and substituting $r = R$, we have:

$$\frac{\partial y}{\partial n}(R,\theta) = -\sum_{n=0}^{\infty}{}' \int_0^{2\pi} m_n(\theta-\theta')\, y(R,\theta')\, d\theta' \tag{2.9}$$

$$m_n(\theta) = -\frac{k}{\pi}\frac{H_n^{(1)\prime}(kR)}{H_n^{(1)}(kR)}\cos n\theta. \tag{2.10}$$

Then the boundary condition verified on ∂D is an integrodifferential Dirichlet-Neumann condition:

$$\frac{\partial y_S}{\partial n} = -\mathcal{M} y_S \text{ on } \partial D, \tag{2.11}$$

$$\mathcal{M} y_S(R,\theta) = \sum_{n=0}^{\infty}{}' \int_0^{2\pi} m_n(\theta-\theta')\, y_S(R,\theta')\, d\theta'. \tag{2.12}$$

Relations (2.2) and (2.7) can be used to compute the radiation diagram, once we know the values of diffracted wave y on ∂D. For r large enough, we have indeed

$$\sqrt{r} \mid y(r,\theta) \mid \approx A(\theta). \tag{2.13}$$

Then we compute the radiation in the sector $\Theta = [\theta_1, \theta_2]$ by

$$\int_\Theta \mid y(r,\theta) \mid^2 \, d\theta. \tag{2.14}$$

It is easier to work with homogeneous conditions at the border $\partial\mathcal{S}$. We introduce $w_\mathcal{S} = y_\mathcal{S} + z$, the total wave (incident and diffracted wave). We see that the total wave is solution of the following system of equations:

$$\begin{cases} \Delta w_\mathcal{S} + k^2 w_\mathcal{S} = 0 & \text{in } \Omega \\ w_\mathcal{S} = 0 & \text{on } \Gamma \\ \frac{\partial w_\mathcal{S}}{\partial n} = -\mathcal{M} w_\mathcal{S} + (\mathcal{M} z + \frac{\partial z}{\partial n}) & \text{on } \partial D \, . \end{cases} \tag{2.15}$$

3 The cost functional

The radiation at infinity is computed from the values of $y_\mathcal{S}$ on ∂D. Let $\mathcal{O}$ be an open set of regular boundary such that:

$$\mathcal{S} \subset \mathcal{O} \subset D, \ \forall \mathcal{S} \in \mathcal{S}_{ad} \tag{3.1}$$

$$\Theta \subset \partial D. \tag{3.2}$$

Assume that the disk radius R is large enough. The radiation at infinity in a direction $\theta \in [0, 2\pi]$ can be approximated by $\mid y_\mathcal{S}(R,\theta) \mid$. Then, for minimizing the radiation at infinity in the arc $[\theta_1, \theta_2]$ we introduce the cost functional j defined by

$$j(\mathcal{S}) = \int_{\theta_1}^{\theta_2} \mid y_\mathcal{S}(R,\theta) \mid^2 \, d\theta = \int_\Theta \mid y_\mathcal{S} \mid^2 \, d\Theta. \tag{3.3}$$

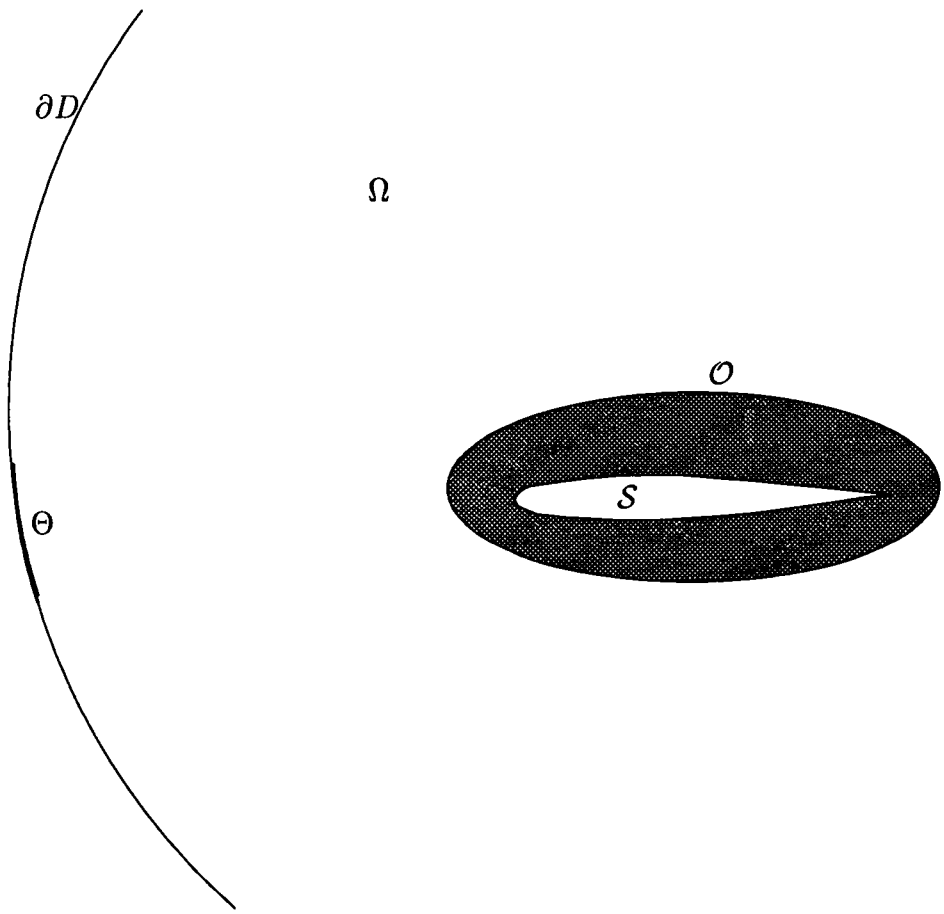

Figure 3.1: The observation region

4 Differentiability of wave problem

To characterize the optimum domain that minimizes the radar visibility, and to compute descent directions of the cost function like in optimal control theory, we must conveniently express the idea of variation of the state and the cost function with respect to the domain. To do this, we need to introduce some vector space structure associated to the set of feasible domains, which are our control variables.
Here we use the method of distributed variations, that briefly, consists at the following: We consider an initial domain $\Omega \in \Re^n$ ($n = 2$ in our 2D problem). For

$$u : \Re^n \longrightarrow \Re^n$$

vector of displacements in $\Re^n$, we define

$$\Omega + u = \{x + u(x),\ x \in \Omega\}$$

Then we consider the elements u as variations of Ω and we define the "derivative of j with respect to Ω" as follows:

$$u \longrightarrow \Omega + u \longrightarrow y_{\Omega+u} \longrightarrow j(\Omega + u) = J(\Omega + u, y_{\Omega+u}) \tag{4.1}$$

Now, the control variable is u defined on a vector space, and we look for a development of the form:

$$j(\Omega + u) = j(\Omega) + L(u) + \cdots \tag{4.2}$$

or equivalently

$$j(\Omega + u) = j(\Omega) + j'(\Omega; u) + o(u). \tag{4.3}$$

Here $L = j'(\Omega)$ is a linear mapping, and is the derivative of j with respect to Ω, and o is such that

$$\lim_{|v| \to 0} \frac{o(v)}{|\ v\ |} = 0 \tag{4.4}$$

4.1 Domain variations

In [3] we find the following lemma:

Lemma 1 *For every $k \geq 1$, there is $\epsilon_k > 0$ such that if $u \in W^{k,\infty}(\Re^n)$ and $\|u\|_{k,\infty} \leq \epsilon_k$ then:*

i) $I + u : \Re^n \longrightarrow \Re^n$ *is bijective;*

ii) $(I + u)^{-1} \in W^{2,\infty}(\Re^n)$.

We use this lemma with $k = 2$, $n = 2$, $\epsilon = \epsilon_2$ and we define the set of variations of Ω (or equivalently $\mathcal{S}$)

$$U = \left\{ u \in W^{2,\infty}\left(\Re^2\right),\ \|u\|_{2,\infty} \leq \epsilon,\ u = 0 \text{ in } \Re^2 - \mathcal{O} \right\} \tag{4.5}$$

It yields from lemma (1) that

$$I + u : \Omega \longrightarrow \Omega + u = \{x + u(x),\ x \in \Omega\} \tag{4.6}$$

is bijective. We impose $u = 0$ in $\Re^2 - \mathcal{O}$ to ensure that the feasible airfoils are contained in a bounded region $\mathcal{O}$. Then the observation region Θ has no intersection with any $\mathcal{S} \in \mathcal{S}_{ad}$. So $y_{S|\Theta}$ is always defined.
Let us suppose that $\{\Omega + u,\ u \in U\} \subset \Omega_{ad}$, that is, "$\Omega$ is an interior point of Ω_{ad}".
It yields also from lemma (1) that for all $u \in U$ the matrix $[\partial_j (I + u)_i]$ is invertible. We denote by $M(u)$ the matrix

$$[M_{ij}(u)] = [\partial_j (I + u)_i]^{-t} \tag{4.7}$$

In what follows we need the following results (see [3]):

Lemma 2 *If $u \in W^{k,\infty}(\Re^n)$, $k \geq 1$, $\|u\|_{k,\infty} < \frac{1}{2}$, and $f \in W^{1,1}(\Re^n)$, then*

$$(\nabla f) \circ (I + u) = M(u) \nabla (f \circ (I + u)) \tag{4.8}$$

Lemma 3 *For all $k \geq 1$, the application*

$$\begin{array}{rcl} W^{k,\infty}(\Re^n) & \longrightarrow & W^{k-1,\infty}(\Re^n) \\ u & \longmapsto & \nabla(I + u)^{-1} = [\partial_j (I + u)_i]^{-t} = M(u) \end{array}$$

defined for $\|u\| \leq \epsilon_k$ is continuously differentiable in a neighborhood of 0. Its derivative in 0 in the direction u is ${}^t[D_j u_i]$.

4.2 Computation of the derivative

Let $g \in C^\infty\left(\Re^N\right)$ be the solution of

$$\left\{ \begin{array}{rcll} \Delta g + k^2 g & = & 0 & \text{in } \Re^2 - \mathcal{O} \\ g & = & 0 & \text{in } \mathcal{O} \\ \frac{\partial g}{\partial n} & = & -\mathcal{M} g + (\mathcal{M} z + \frac{\partial z}{\partial n}) & \text{on } \partial D. \end{array} \right. \tag{4.9}$$

We consider the problem:

$$\min_{u\in U} E(u) = \int_{\Theta} \mid w(u) - z \mid^2 \, d\theta \tag{4.10}$$

where $w(u)$ is the total wave, solution of Helmholtz equation for the domain $\mathcal{S} + u$:

$$\left\{ \begin{array}{rcll} \Delta w(u) + k^2 w(u) & = & 0 & \text{in } (\Omega + u) \\ w(u) & = & 0 & \text{on } \Gamma + u \\ \frac{\partial w(u)}{\partial n} & = & -\mathcal{M} w(u) + (\mathcal{M} z + \frac{\partial z}{\partial n}) & \text{on } \partial D. \end{array} \right. \tag{4.11}$$

We see that by definition:

$$w(u) = w_{\mathcal{S}+u} \quad ; \quad w(0) = w_{\mathcal{S}} \tag{4.12}$$

$$E(u) = j(\mathcal{S} + u) \quad ; \quad E(0) = j(\mathcal{S}) \tag{4.13}$$

for every variation $u \in U$. That is, j and E represents the same cost function with the difference that the second one is written on a set U with a local vector space structure convenient for differentiation.
From [16][18] we have the following theorem

Theorem 1 *There is only one solution $w(u)$ of the problem (4.11), and it is in $H^2(\Omega + u)$.*

We now look for $u^* \in U$ such that $E(u^*) \leq E(u)$ for all $u \in U$.
For that, we are interested in the existence and computation of a Frechet derivative of the function

$$\begin{array}{rcl} E : U & \longrightarrow & \Re \\ u & \longmapsto & E(u). \end{array} \tag{4.14}$$

Theorem 2 *The application*

$$\begin{array}{rcl} U & \longrightarrow & H^2(\Omega) \\ u & \longmapsto & w(u) \circ (I + u) \end{array} \tag{4.15}$$

is differentiable in 0.

Proof: We define the spaces:

$$W_* = \left\{ v \in H^2(\Omega) \, : \, v = 0 \text{ on } \partial\mathcal{S}, \, \frac{\partial v}{\partial n} = -\mathcal{M} v + \left(\mathcal{M} z + \frac{\partial z}{\partial n} \right) \right\}$$

$$V_* = \left\{ y \in H^2(\Omega) \, : \, y = 0 \text{ on } \partial\mathcal{S}, \, \frac{\partial y}{\partial n} = -\mathcal{M} y \right\}.$$

Then we can write $W_* = g + V_*$.

i) **The equation satisfied by** $w(u) \circ (I+u)$

For $u \in U$, $w(u) \in H^2(\Omega + u)$ is solution of

$$\begin{cases} [\Delta w(u) + k^2 w(u)] \circ (I+u) = 0 & \text{in } \Omega \\ w(u) \circ (I+u) = 0 & \text{on } \Gamma \\ \dfrac{\partial w(u)}{\partial n} = -\mathcal{M} w(u) + (\mathcal{M} z + \dfrac{\partial z}{\partial n}) & \text{on } \partial D \end{cases} \tag{4.16}$$

Then $w(u) \circ (I+u) \in W^*$ and this implies the existence of $v(u) \in V_*$ such that

$$w(u) \circ (I+u) = g + v(u). \tag{4.17}$$

We now define an application $F : U \times V_* \longrightarrow L^2(\Omega)$ by

$$F(u,v) = \left\{\Delta\left[(v+g) \circ (I+u)^{-1}\right]\right\} \circ (I+u) + k^2(v+g). \tag{4.18}$$

Then by definition of F we have

$$F(u, v(u)) = \left[\Delta w(u) + k^2 w(u)\right] \circ (I+u) = 0 \tag{4.19}$$

In other words, v is the variation of the solution of the P.D.E. with respect to u when the domain is changed and $F = 0$.

So (4.17) can be written as:

$$F(u, v(u)) = \left[\Delta w(u) + k^2 w(u)\right] \circ (I+u) = 0 \tag{4.20}$$

ii) **Differentiability of** F.

Lemmas (2)(3) show that F is well defined, continuously differentiable in a neighborhood of $(0, v(0))$ in $U \times V_*$ and yield the expression that follows:

$$\begin{aligned} F(u,v) &= \left\{\Delta\left[(v+g) \circ (I+u)^{-1}\right]\right\} \circ (I+u) + k^2(v+g) \\ &= T_r \nabla \left\{\nabla\left[(v+g) \circ (I+u)^{-1}\right]\right\} \circ (I+u) + k^2(v+g) \\ &= T_r \left[M(u) \nabla \left\{\nabla\left[(v+g) \circ (I+u)^{-1}\right] \circ (I+u)\right\}\right] + k^2(v+g) \\ &= T_r \left\{M(u) \nabla \left[M(u) \nabla (v+g)\right]\right\} k^2(v+g). \end{aligned} \tag{4.21}$$

iii) $\partial F/\partial v$ **is an isomorphism.**

Let $u \in U$ and $v, \overline{v} \in V^*$. Then

$$\begin{aligned} \frac{\partial F}{\partial v}(u,v)\cdot\overline{v} &= T_r\left\{M(u)\nabla\left[M(u)\nabla\overline{v}\right]\right\} + k^2\overline{v} \\ &= \left\{\Delta\left[\overline{v}\circ(I+u)^{-1}\right]\right\}\circ(I+u) + k^2\overline{v}. \end{aligned} \tag{4.22}$$

(4.23)

Then we have that

$$\frac{\partial F}{\partial v}(0, v(0)) = \Delta + k^2 Id, \tag{4.24}$$

and this is an isomorphism between the two spaces (see [16]).

iv) **Application of Implicit Function Theorem**

From i), ii) and iii), the Implicit Function Theorem concludes that there are:

- O_1 neighborhood of 0 in U,
- O_2 neighborhood of $v(0)$ in V_*,
- $v : O_1 \longrightarrow V_*$ continuously differentiable

such that

$$\{(u,v) \in O_1 \times O_2 \ : \ F(u,v) = 0\} = \{(u, v(u)) \in O_1 \times V_*\}. \tag{4.25}$$

That is, for all $u \in O_1$, there exists $v = v(u) \in V_*$, verifiying $F(u, v(u)) = 0$. Setting

$$w(u) = [v(u) + g] \circ (I+u)^{-1} \tag{4.26}$$

this says that the application:

$$\begin{array}{rccc} H : & O_1 & \longrightarrow & H^2(\Omega) \subset H^1(\Omega) \\ & u & \longmapsto & w(u)\circ(I+u) = g + v(u) \end{array} \tag{4.27}$$

exists and is continuously differentiable in 0.

Definition 1 *We note $w'(\overline{u})$ the derivative of the above application H at the origin $u = 0$, in the direction of $\overline{u}$*

$$w'(\overline{u}) = H'(0;\overline{u}). \tag{4.28}$$

This is the so-called ***local derivative.***

We see that $H'(0;\overline{u}) = v'(0;\overline{u}) = w^{\cdot}(\overline{u})$ and then, the implicit function theorem implies that

$$w^{\cdot}(u) = -\left(\frac{\partial F}{\partial v}(0;v(0))\right)^{-1} \frac{\partial F}{\partial u}(0;v(0))(u); \tag{4.29}$$

that is

$$\Delta w^{\cdot}(u) + k^2 w.^{(}u) = -\frac{\partial F}{\partial u}(0;v(0))(u). \tag{4.30}$$

In [3] we have that existence of local derivative implies existence of a derivative at $u = 0$ for all applications

$$u \longrightarrow w(u)_{|\omega} \tag{4.31}$$

for every $\omega \subset\subset \Omega$.

Definition 2 *The derivative of these application is called* ***global derivative*** *and we denote by $w'(\overline{u})$ the global derivative in the direction $\overline{u}$.*

We find in [2], the relation between local and global derivative:

$$w'(\overline{u}) = w^{\cdot}(\overline{u}) - \overline{u}\,\nabla w(0) \tag{4.32}$$

We now proceed to the calculation of $w'(\overline{u})$. We first have:

Proposition 1

$$-\frac{\partial F}{\partial u}(0;v(0))\,\overline{u} = \Delta\left(\overline{u}\,\nabla w(0)\right) + k^2\left(u\,\nabla w(0)\right). \tag{4.33}$$

Proof: Let $u, \overline{u} \in U$ and $v \in V^*$. Then

$$\begin{aligned} -\frac{\partial F}{\partial u}(u,v)\cdot\overline{u} &= T_r\left\{M(u)\,\nabla\overline{u}\,M(u)\,\nabla\left[M(u)\,\nabla(v+g)\right]\right\} \\ &+ T_r\left\{M(u)\,\nabla\left[M(u)\,\nabla\overline{u}\,M(u)\,\nabla(v+g)\right]\right\}. \end{aligned} \tag{4.34}$$

Then, we have in one hand:

$$\begin{aligned} -\frac{\partial F}{\partial u}(0,v(0))\,\overline{u} &= T_r\left\{\nabla\overline{u}\,\nabla\left[\nabla\left(v(0)+g\right)\right] + \nabla\left[\nabla\overline{u}\,\nabla\left(v(0)+g\right)\right]\right\} \\ &= T_r\left\{\nabla\overline{u}\,\nabla\left[\nabla w(0)\right] + \nabla\left[\nabla\overline{u}\,\nabla w(0)\right]\right\} \\ &= \sum_{i,j=1}^{n=2}\left(\partial_{ii}\overline{u}_j\partial_j w(0) + 2\partial_i\overline{u}_j\partial_{ij}w(0)\right). \end{aligned} \tag{4.35}$$

(4.36)

On the other hand:

$$\begin{aligned}
&\Delta(\overline{u}\,\nabla w(0)) + k^2(\overline{u}\,\nabla w(0)) = \\
&= T_r\{\nabla[\nabla(\overline{u}\,\nabla w(0))]\} + k^2[\overline{u}\,\nabla w(0)] \\
&= T_r\{\nabla[\nabla\overline{u}\,\nabla w(0) + \nabla(\nabla w(0))\,\overline{u}]\} + \sum_{j=1}^{n} k^2\,\partial_j w(0)\,\overline{u}_j \\
&= \sum_{i,j=1}^{n}(\partial_{ii}\overline{u}_j\partial_j w(0) + 2\partial_i\overline{u}_j\partial_{ij}w(0)) + \sum_{j=1}^{n}\partial_j\underbrace{\left(\sum_{i=1}^{n}\partial_{ii}w(0) + k^2 w(0)\right)}_{=0 \text{ from } (4.17)(4.16)}\overline{u}_j. \quad (4.37)
\end{aligned}$$

(4.38)

We now go back to the calculation on $w'(\overline{u})$. Considering that $w(0) = w_S$ it follows from last proposition and relations (4.32)-(4.30) that for all directions $\overline{u} \in U$,

$$\Delta w^{\cdot}(\overline{u}) + k^2 w^{\cdot}(\overline{u}) = \Delta(\overline{u}\,\nabla w_S) + k^2\,\overline{u}\,\nabla w_S \quad (4.39)$$

$$\Delta w'(\overline{u}) + k^2 w'(\overline{u}) = 0. \quad (4.40)$$

At the boundary the following conditions are easily verified:

$$v(u) = w(u) \circ (I + u) = 0 \text{ on } \Gamma \qquad \forall u \in U, \quad (4.41)$$

and then for $u = 0$, we have at all directions $\overline{u} \in U$ that

$$v'(0;\overline{u}) = w^{\cdot}(\overline{u}) = 0 \text{ on } \Gamma \quad (4.42)$$

From (4.32) we have

$$w'(\overline{u}) = w^{\cdot}(\overline{u}) - \overline{u}\,\nabla w_S = -\overline{u}\,\nabla w_S \text{ on } \Gamma. \quad (4.43)$$

But $w_S = 0$ on Γ, then

$$\nabla w_S = \frac{\partial w_S}{\partial n}\,n, \quad (4.44)$$

and thus

$$w'(\overline{u}) = -\overline{u}_n\,\frac{\partial w_S}{\partial n}. \quad (4.45)$$

Here $\overline{u}_n$ is the composant of $\overline{u}$ in the normal direction $\vec{n}$, $\overline{u}_n = \overline{u} \cdot \vec{n}$.
By definition, $u = 0$ in $R^2 - \mathcal{O}$ for all $u \in U$, then for the absorbing boundary we have that $H(u) = w(u)$ at the points close to ∂D. Thus

$$\begin{aligned}\frac{\partial H(u)}{\partial n} &= \frac{\partial w(u)}{\partial n} \\ &= -\mathcal{M}w(u) + (\mathcal{M}z + \frac{\partial z}{\partial n}) \\ &= -\mathcal{M}H(u) + (\mathcal{M}z + \frac{\partial z}{\partial n}).\end{aligned} \tag{4.46}$$

and that implies:

$$\frac{\partial w^{\cdot}(\overline{u})}{\partial n} = -\mathcal{M}w^{\cdot}(\overline{u}) \text{ on } \partial D \tag{4.47}$$

Thus the relations (4.32) and (4.47) yield

$$\begin{aligned}\frac{\partial w'(\overline{u})}{\partial n} &= \frac{\partial w^{\cdot}(\overline{u})}{\partial n} - \overline{u}\,\nabla w_{\mathcal{S}} \\ &= \frac{\partial w^{\cdot}(\overline{u})}{\partial n} \\ &= -\mathcal{M}w^{\cdot}(\overline{u}) \\ &= -\mathcal{M}w'(\overline{u}).\end{aligned} \tag{4.48}$$

Of relations (4.40)-(4.47) we conclude the following result:

Theorem 3 *For all $u \in U$ we have:*

$$\left\{\begin{array}{rcll}\Delta w'(\overline{u}) + k^2 w'(\overline{u}) &=& 0 & in\ \Omega \\ w'(\overline{u}) &=& -\frac{\partial w_{\mathcal{S}}}{\partial n} \cdot \overline{u}_n & on\ \Gamma \\ \frac{\partial w'(\overline{u})}{\partial n} &=& -\mathcal{M}w'(\overline{u}) & on\ \partial D\end{array}\right. \tag{4.49}$$

We have then, the differentiability of the state w. Let us study now the differentiability of the cost functional.

Lemma 4 *The application*

$$\begin{array}{rcl}K : U & \longrightarrow & W^{1,1}(\Omega) \\ u & \longrightarrow & \mid w(u) \circ (I+u) - g \mid^2\end{array} \tag{4.50}$$

is differentiable at all points and

$$K'(u) \cdot v = 2\,Re\left\{[w(u) \circ (I+u) - g] \cdot \overline{w^{\cdot}(u)}\right\},\ \forall v \in U. \tag{4.51}$$

Proof: It is only necessary to write:

$$\begin{array}{ccccc} U & \longrightarrow & H^1(\Omega) & \longrightarrow & W^{1,1}(\Omega) \\ u & \longrightarrow & w(u) \circ (I+u) - g & \longrightarrow & \mid w(u) \circ (I+u) - g \mid^2 \end{array} \tag{4.52}$$

to see that K is composition of differentiable applications.

From this lemma, we deduce:

Theorem 4 *The cost function*

$$\begin{array}{rccc} j : & U & \longrightarrow & \Re \\ & u & \longrightarrow & \int_\Theta \mid w(u) - g \mid^2 \, d\theta \end{array} \tag{4.53}$$

is differentiable. The derivative at 0 *in the direction* $u \in U$ *is*

$$j'(0)\, u = 2 \int_\Theta Re \left[(w-g) \cdot \overline{w'(u_n)} \right] d\theta \tag{4.54}$$

4.3 Optimality Conditions

We know that the derivative $j'(0)$ with respect to variations u of $\mathcal{S}$ is related to the optimality conditions.
Now we look for a more suitable expression for $j'(0) \cdot u$ that may give a valuable interpretation for the optimality conditions and for the computation of descent directions.

Theorem 5 *Let* $p \in H^1(\Omega)$ *such that*

$$p_{|\Gamma} = 0, \tag{4.55}$$

$$\int_\Omega [\nabla \phi \cdot \nabla p - k^2 \phi \cdot p] \, dx + \int_{\partial D} (\mathcal{M}\phi) \cdot p = 2\, Re \int_\Theta (w-g) \bar{\phi} \, d\theta \tag{4.56}$$

for all $\phi \in H^1(\Omega)$ *such that* $\phi = 0$ *on* Γ.
Then for all $u \in U$ *we have*

$$j'(0)\, u = \int_\Gamma \frac{\partial p}{\partial n} \cdot \frac{\partial w_{\mathcal{S}}}{\partial n} \cdot u_n \, d\Gamma. \tag{4.57}$$

Proof: From (4.56), we first have

$$\begin{aligned} &\int_\Omega \left[\nabla w'(u) \, \nabla p - k^2 \, p \, w'(u) \right] dx = \\ &= -\int_{\partial D} \mathcal{M} w'(u) \; p + 2\, Re \int_\Theta (w_{\mathcal{S}} - g) \, \overline{w'(u)} \, d\theta + \int_\Gamma \frac{\partial p}{\partial n} \, w'(u) \, d\Gamma. \end{aligned} \tag{4.58}$$

On the other hand, writing (4.49) under a variational form, we get

$$\begin{aligned}
&\int_\Omega \left[\nabla w'(u)\,\nabla p - k^2\, p\, w'(u)\right]\, dx = \\
&= -\int_\Omega \left[\Delta w'(u) + k^2\, w'(u)\right]\, p\, dx - \int_{\partial D} \mathcal{M} w'(u)\, p \\
&= -\int_{\partial D} \mathcal{M} w'(u)\, p. \qquad (4.59)
\end{aligned}$$

By substraction, and from (4.49), we deduce

$$\begin{aligned}
j'(0)\,u &= 2\,Re \int_\Theta (w-g)\,\overline{w'(u)} d\theta \qquad (4.60)\\
&= -\int_\Gamma \frac{\partial p}{\partial n}\, w'(u)\, d\Gamma \qquad (4.61)\\
&= \int_\Gamma \frac{\partial p}{\partial n}\frac{\partial w_S}{\partial n}\, u_n\, d\Gamma. \qquad (4.62)
\end{aligned}$$

5 Discretization of wave problem

Let $z(\vec{x}) = e^{i\vec{\omega}\cdot\vec{x}}$ the plane incident wave. For $u \in U$, we have that the diffracted wave w_u is the solution of

$$\begin{cases} \Delta w_u + k^2 w_u &= 0 & \text{in } \Omega + u \\ w_u &= 0 & \text{on } \Gamma + u \\ \frac{\partial w_u}{\partial n} &= -\mathcal{M} w_u + (\mathcal{M} z + \frac{\partial z}{\partial n}) & \text{on } \partial D, \end{cases} \tag{5.1}$$

and the objective is to minimize

$$\min_{u \in U} E(u) = \int_\Theta |w_u - z|^2 \, d\theta \tag{5.2}$$

5.1 Discrete state equation

We use a finite element method. First we replace (5.1) by its variational formulation

$$\int_{\Omega+u} [\nabla w_u \cdot \nabla \phi - k^2 w_u \cdot \phi] \, d\Omega + \int_{\partial D} \mathcal{M} w_u \cdot \phi = \int_{\partial D} (\mathcal{M} z + \frac{\partial z}{\partial n}) \cdot \phi \tag{5.3}$$

for all $\phi \in H^1(\Omega + u)$, $\phi = 0$ on $\Gamma + u$.

At the discret level, let u_h be the discrete displacements corresponding to the discretization of the domain $\Omega + u$ by Ω_{u_h}, with a mesh

$$[\Omega_{u_h}] = (\Xi_h, X_{u_h}) \, . \tag{5.4}$$

Above, Ξ_h is topology of the mesh, which is made of triangles and quadrangles (and is independent of u_h) and X_{u_h} is the vector of mesh coordinates.

Let $H^1_{0u_h}$ be the space of piecewise polynomial functions of degre 1 in Ω_{u_h} associated to the mesh $[\Omega_{u_h}]$ which vanishes on $\partial \mathcal{S}_{u_h}$, the interior boundary of Ω_{u_h}.

The approximation of w_u is given by $w_{u_h} \in H^1_{0u_h}$ solution of

$$\int_{\Omega_{u_h}} [\nabla w_{u_h} \cdot \nabla \phi_h - k^2 w_{u_h} \cdot \phi_h] \, d\Omega + \int_{\partial D_h} \mathcal{M}_h w_{u_h} \cdot \phi_h = \int_{\partial D_h} \left(\mathcal{M}_h z + \frac{\partial z}{\partial n} \right)_h \cdot \phi_h \tag{5.5}$$

for all $\phi_h \in H^1_{0u_h}$, where $\mathcal{M}_h$ and $\left(\mathcal{M}_h z + \frac{\partial z}{\partial n} \right)_h$, are discrete approximations on ∂D_h of $\mathcal{M}$ and $\left(\mathcal{M} z + \frac{\partial z}{\partial n} \right)$, respectively.

Let n_h the dimension of $H^1_{0u_h}$, and $q_j^{u_h}$ its finite element basis, associated to the mesh $[\Omega_{u_h}]$.

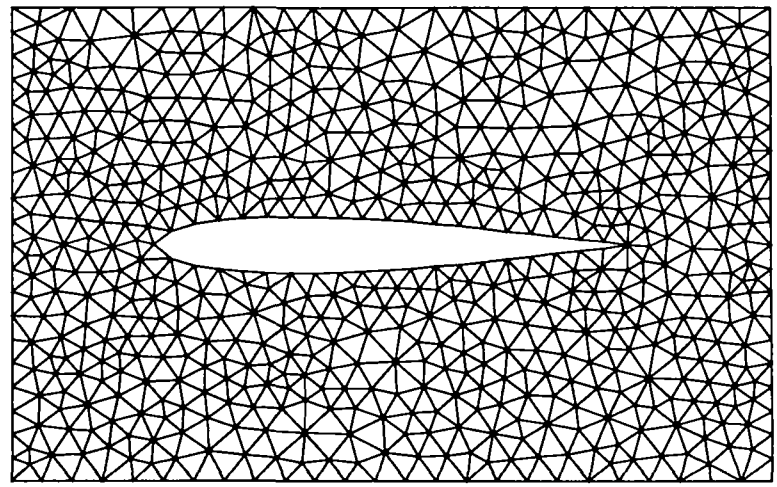

Figure 5.1: Mesh close to the airfoil

The approximate solution being of the form

$$w_{u_h} = \sum_{j=1}^{n_h} W_j^{u_h} \cdot q_j^{u_h}, \tag{5.6}$$

we get the finite dimensional linear system of grid equations

$$\int_{\Omega_{u_h}} [\nabla w_{u_h} \cdot \nabla q_j^{u_h} - k^2 w_{u_h} \cdot q_j^{u_h}]\, d\Omega_h + \int_{\partial D_h} \mathcal{M}_h w_{u_h} \cdot q_j^{u_h} = \int_{\partial D_h} \left(\mathcal{M}_h z + \frac{\partial z}{\partial n} \right)_h \cdot q_j^{u_h}, \tag{5.7}$$

for all $j = 1, \cdots, n_h$. This is equivalent to

$$A_{ij}^{u_h} W_j^{u_h} = B_i^{u_h} \quad , i = 1, \ldots, n_h, \tag{5.8}$$

where $A^{u_h} = \left[A_{ij}^{u_h}\right] \in M_{n_h}(C)$, $B^{u_h} = [B_i^{u_h}] \in M_{n_h \times 1}(C)$, $W_{u_h} = [W_i^{u_h}] \in M_{n_h \times 1}(C)$,

$$\begin{aligned} A_{ij}^{u_h} &= \int_{\Omega_{u_h}} [\nabla q_i^{u_h} \cdot \nabla q_j^{u_h} - k^2 q_i^{u_h} \cdot q_j^{u_h}]\, d\Omega_h + \int_{\partial D_h} \mathcal{M}_h q_i^{u_h} \cdot q_j^{u_h} \\ B_i^{u_h} &= \int_{\partial D_h} \left(\mathcal{M}_h z + \frac{\partial z}{\partial n} \right)_h \cdot q_i^{u_h}. \end{aligned}$$

For the optimization problem we have a certain number of moving mesh points. They are the points on the interior boundary Γ_h and perhaps their neighbors. Let $\sigma = (\sigma_1, \ldots, \sigma_K)$ be the vector that describes the coordinates of these moving mesh points.

We fix the other mesh points, i.e., the points not closed to Γ_h. In fact, for the analysis is sufficient that the points closed to the absorbing boundary ∂D_h and to the observation region Θ_h be fixed once for all.

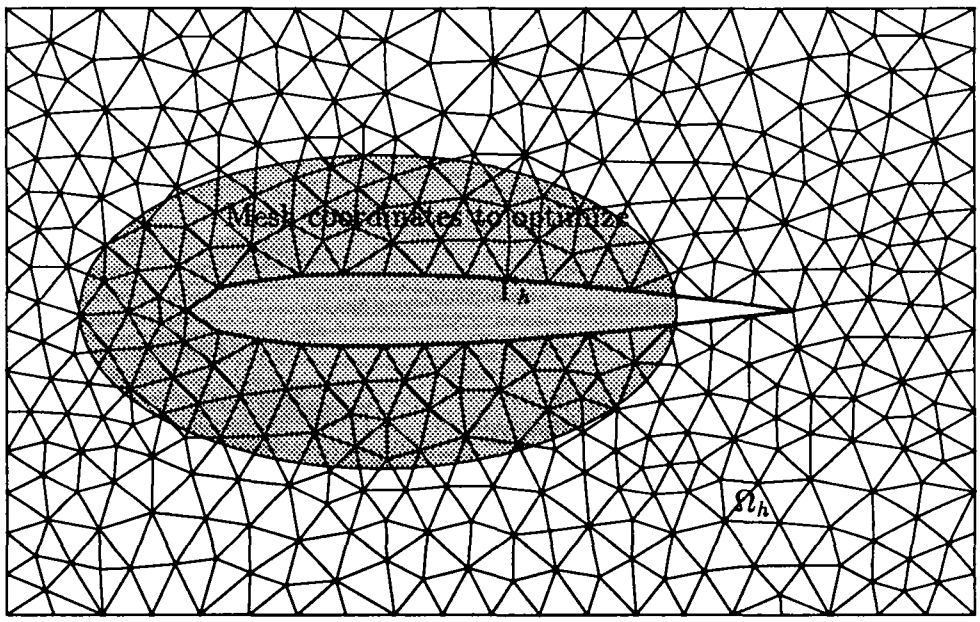

Figure 5.2: The points to optimize

Then for every σ vector of coordinates of mesh moving points we have the corresponding discrete displacements vector $u_h(\sigma)$, and the scheme:

$$\sigma \longrightarrow u_h(\sigma) \longrightarrow w_{u_h(\sigma)} \longrightarrow j_h(\sigma) = J_h\left(w_{u_h(\sigma)}\right) \tag{5.9}$$

We define the nonlinear constrained finite dimensional optimization problem

$$\min_{\sigma} j_h(\sigma) \stackrel{def}{=} J_h\left(w_{u_h(\sigma)}\right) \stackrel{def}{=} \int_{\Theta_h} |w_{u_h(\sigma)} - z|^2 \, d\theta. \tag{5.10}$$

The contraints of the problems are not classical and hard to describe, because they are related with the non degeneration of the mesh. We forget for a moment the contraints and for an admissible σ, we are interested at the gradient $\nabla j_h(\sigma)$, to be used in a descent algorithm for optimization.

Looking at (5.8) we have that $j_h(\sigma)$ depends on σ by means of the solution of a linear system whose coefficients depends on σ.

Let us write explicitly where are the dependencies on σ. The points near ∂D_h and of the observation region Θ_h do not move. Thus the basis functions associated to these

points are noted q_i^h because they do not change with σ. Let I_Θ be the set of index of mesh points close to the observation region

$$I_\Theta = \left\{ i = 1, \ldots, n_h \,:\, q_i^h \cap \Theta_h \neq \oslash \right\}. \tag{5.11}$$

Let $[W_i(\sigma)] = \left[W_i^{u_h(\sigma)}\right]$. We obtain the following quadratic expression of $j_h(\sigma)$ in terms of $[W_i(\sigma)]$:

$$\begin{aligned} j_h(\sigma) &= \frac{1}{2}\int_{\Theta_h} |w^h - z|^2 \, d\theta \\ &= \frac{1}{2}\int_{\Theta_h} |\sum_{i\in I_\Theta} W_i(\sigma) q_i^h - z|^2 \, d\theta \\ &= \frac{1}{2}\sum_{i,j\in I_\Theta} W_i(\sigma)\overline{W_j(\sigma)} \int_{\Theta_h} q_i^h q_j^h - Re\left[\sum_{i\in I_\Theta} W_i(\sigma)\int_{\Theta_h} q_i^h \overline{z}\, d\theta\right] + \int_{\Theta_h} |z|^2 \, d\theta \\ &= \frac{1}{2}\overline{W}^t(\sigma)\cdot C \cdot W(\sigma) + Re\left[D^t \cdot W(\sigma)\right] + C_0, \end{aligned}$$

where $C = [C_{ij}] \in M_{n_h}(\Re)$, $D = [D_i] \in M_{n_h \times 1}(C)$, $C_0 \in \Re$ are independent of σ, that is, they depend on the fixed part of the mesh, but not on the moving points. More precisely, we have

$$\begin{aligned} C_{ij} &= \begin{cases} \int_{\Theta_h} q_i^h q_j^h & \text{if } i,j \in I_\Theta \\ 0 & \text{if not} \end{cases} \\ D_i &= \begin{cases} \int_{\Theta_h} q_i^h \overline{z} & \text{if } i \in I_\Theta \\ 0 & \text{if not} \end{cases} \\ C_0 &= \int_{\Theta_h} |z|^2. \end{aligned}$$

Above, $W(\sigma)$ is solution of

$$A(\sigma)\cdot W(\sigma) = B(\sigma), \tag{5.12}$$

where $A(\sigma) = A^{u_h(\sigma)}$ and $B(\sigma) = B^{u_h(\sigma)}$ are respectively the matrix of left and right hand side corresponding to the system of linear equations (5.8) associated to σ.

5.2 Computation of the gradient of cost function

We treat the linear system (5.8) like a set of constraints and we define the Lagrangian

$$\mathcal{L} : \Re^K \times M_{n_h \times 1}(C) \times M_{n_h \times 1}(C) \longrightarrow \Re \tag{5.13}$$

$$\mathcal{L}(\sigma, W, P) = \frac{1}{2} W^t \cdot C \cdot W + Re\left(D^t \cdot W\right) + C_0 + Re\left\{P^t \cdot [A(\sigma) \cdot W - B(\sigma)]\right\}. \tag{5.14}$$

Then the Kuhn-Tucker optimality conditions yield the following:

5.2.1 i) Discrete state equation.

$W(\sigma)$ verifies

$$\frac{D\mathcal{L}}{DP}(\sigma, W(\sigma), P) = 0 \Longleftrightarrow A(\sigma) \cdot W(\sigma) = B(\sigma). \tag{5.15}$$

5.2.2 ii) Discrete adjoint equation.

Let $P(\sigma)$ be, by definition, the adjoint state, solution of the adjoint equation

$$\frac{D\mathcal{L}}{DW}(\sigma, W(\sigma), P(\sigma)) = 0 \Longleftrightarrow A(\sigma)^t \cdot P(\sigma) = C \cdot \overline{W(\sigma)} - D. \tag{5.16}$$

5.2.3 iii) Gradient of the cost function.

We have that

$$j_h(\sigma) = \mathcal{L}(\sigma, W(\sigma), P(\sigma)), \tag{5.17}$$

and then, $\forall k \in \{1, \ldots, K\}$,

$$\begin{aligned}
\frac{\partial j_h}{\partial \sigma_k} &= \frac{\partial \mathcal{L}}{\partial \sigma_k}(\sigma, W(\sigma), P(\sigma)) + \frac{\partial \mathcal{L}}{\partial W}(\sigma, W(\sigma), P(\sigma)) \cdot \frac{\partial W}{\partial \sigma_k} + \frac{\partial \mathcal{L}}{\partial P}(\sigma, W(\sigma), P(\sigma)) \cdot \frac{\partial P}{\partial \sigma_k} \\
&= \frac{\partial \mathcal{L}}{\partial \sigma_k}(\sigma, W(\sigma), P(\sigma)) \\
&= Re\left\{P(\sigma)^t \cdot \left[\frac{\partial A}{\partial \sigma_k}(\sigma) \cdot W(\sigma) - \frac{\partial B}{\partial \sigma_k}(\sigma)\right]\right\}.
\end{aligned}$$

The terms $\frac{\partial A}{\partial \sigma_k}(\sigma)$ and $\frac{\partial B}{\partial \sigma_k}(\sigma)$ are easily and quickly computed, because they depend on the variation of function basis of the mesh. We can also use, in the case of complex basis functions, finite differences approximations to compute them. The computational time for these terms is marginal with respect to the solution of state and adjoint equations. Another instrument to do these computations is to use the automatic differentiators of functions represented by programs [7]. The programs for automatic differentiation will become quickly very useful in optimum design.

5.3 Relation between continuous and discrete problems

Let $u = 0 \in U$, and $p \in H^1(\Omega)$ be the solution of

$$\int_\Omega [\nabla\phi \cdot \nabla p - k^2 \phi \cdot p]\, dx + \int_{\partial D} (\mathcal{M}\phi) \cdot p = 2\, Re \int_\Theta (w_0 - z)\bar{\phi}\, d\theta \tag{5.18}$$

for all $\phi \in H^1(\Omega)$ such that $\phi = 0$ on Γ, $p = 0$ on Γ.
We approximate p on the mesh $[\Omega_h]$ by p_h solution of:

$$\int_{\Omega_h} [\nabla\phi_h \cdot \nabla p_h - k^2 \phi_h \cdot p_h]\, dx + \int_{\partial D_h} (\mathcal{M}_h \phi_h) \cdot p_h = 2\, Re \int_{\Theta_h} (w_{0_h} - z)\bar{\phi}_h\, d\theta, \tag{5.19}$$

$\forall \phi_h \in H^1_{0h}$, $p_h \in H^1_{0h}$, and then we write

$$p_h = \sum_{i=1}^{n_h} P_i^h \cdot q_j^{0_h}. \tag{5.20}$$

Let $P^h = \left[P_i^h\right] \in M_{n_h \times 1}(C)$. We can see that $P^h = P(\sigma_0)$, where σ_0 is the vector of coordinates of fixed mesh points for the discretized initial domain $\Omega_h = \Omega_{0_h}$. Indeed, both vectors are solution of the same linear systems. That is, the approximation of the adjoint of the continuous problem is the adjoint for the discrete problem, and then

$$\frac{\partial j}{\partial \sigma_k} = Re\left\{ P^{h^t} \cdot \left[\frac{D\,A}{D\,\sigma_k}(\sigma_0) \cdot W(\sigma_0) - \frac{D\,B}{D\,\sigma_k}(\sigma_0) \right] \right\}. \tag{5.21}$$

6 The use of splines

We have computed the derivatives of the cost functional with respect to the coordinates of the moving mesh points. A mesh has much more information than is needed for design. In practical cases, the airfoil to optimize is not given by a mesh but by a small number of control points located on the wing profile or by a spline curve. Then we must write the derivatives of functional with respect these new variables, which are in small number, say 20.

Let $s = (s_1, \cdots, s_l)$ represent a curve that describes the wing profile, with l the number of unknowns. We must have a method to build a mesh as a function of this new variables.

A method due to Marrocco [13] is the following:

1. Give an initial s that represents for example a spline.

2. Build an initial mesh $[\Omega_h] = (\Xi_h, X_h)$ where the points on Γ_h are on the spline described by s.

   Let $\mathcal{K}$ the set of mesh points of $[\Omega_h]$ represented by the σ, i.e. the unknowns of the optimization problem. Let $\mathcal{K}_\Gamma$ the subset of points on Γ.

3. For a change of spline s, compute the displacements $\vec{D}_k$ for $k \in \mathcal{K}_\Gamma$, as given from the new spline function.

4. Compute the displacement $\vec{D}_i$ for the rest of interior points $i \in \mathcal{K} - \mathcal{K}_\Gamma$ by

$$\vec{D}_i = \frac{1}{\alpha_i} \sum_{k \in \mathcal{K}_\Gamma} w_k \, \alpha_{ki} \, \vec{D}_k \tag{6.1}$$

   where

   w_k is a weight associated to the point k (e.g. the sum of the length of the two boundary segments containing k);

   $\alpha_{ki} = \frac{1}{d_{ki}^\beta}$ where d_{ki} is the distance betwen points k and i, and β is a parameter related with the "elasticity" of the mesh. For $2 \leq \beta \leq 4$ the mesh moves in a very good way as we show in figures (6.1) (6.2);

   $\alpha_i = \sum_{k \in \mathcal{K}_\Gamma} w_k \, \alpha_{ki}$ is a normalisation factor.

5. Change the coordinates of the points $\mathcal{K}$ in X_h. The mesh topology Ξ_h remain unchanged. Actualize σ accordingly..

This is a very robust method in practice: a mesh that is deformed following (6.1) conserves its topology and seldom degenerates. We also see that the mesh changes are differentiable with respect to the displacement of the boundary points. This is important for the use of chain's rule in the following scheme:

$$s \longrightarrow \sigma(s) \longrightarrow j_h(\sigma(s)) \tag{6.2}$$

However, in the course of optimization process we sometimes need a new mesh. The remeshing is **not a differentiable** operation and then we could have troubles, because we can find that the new mesh have a different number of points and a different topology. Fortunately this does not give big errors in the computation because we work with sufficient accuracy in the approximation of the solution of Helmholtz problem, and thus the influence of the mesh on the descent direction is small.

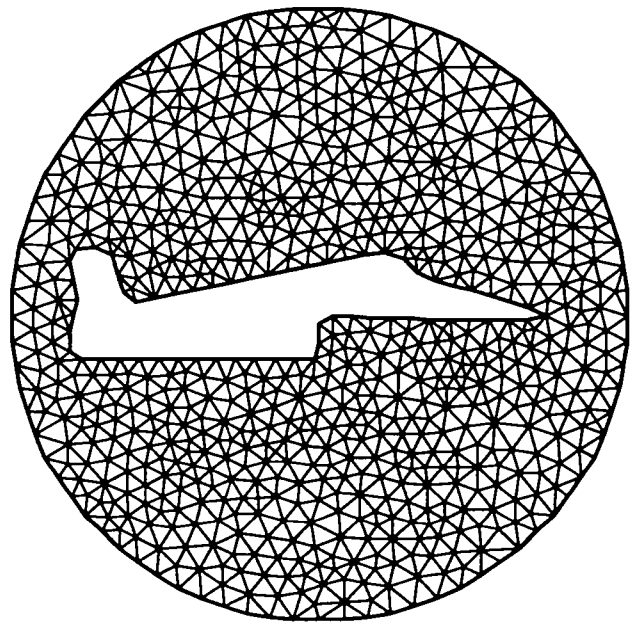

Figure 6.1: Initial mesh

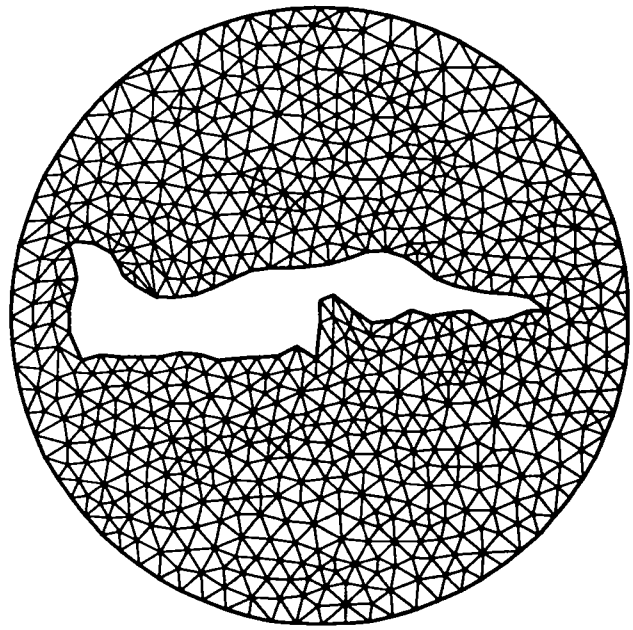

Figure 6.2: Deformed mesh

7 The aerodynamic constraint

For a perfect incompressible fluid, the velocity field satisfies

$$\nabla \cdot \vec{u} = 0, \tag{7.1}$$
$$\nabla \times \vec{u} = 0. \tag{7.2}$$

The flow around a wing profile $\mathcal{S}$ at rest in an unbounded fluid at constant speed at infinity $\vec{u}_\infty$ is approximated numerically by a flow in a bounded domain Ω with an outer boundary Γ_∞, sufficiently far from the airfoil boundary Γ. So Ω is a two dimensional domain with boundary $\partial\Omega = \Gamma \cup \Gamma_\infty$.
The wake is modeled by a stream line Σ issued from the trailing edge P behind $\mathcal{S}$. The flow is not irrotational in the wake, so (7.1) , (7.2) hold in $\Omega - \Sigma$. The boundary conditions on Σ are

$$\vec{u} \cdot n_\Sigma = 0 \text{ on } \Sigma, \ \Sigma \text{ is a streamline}, \tag{7.3}$$
$$\nabla \times \vec{u} \cdot n_\Sigma = 0 \text{ on } \Sigma, \ \text{Vorticity is parallel to } \Sigma, \tag{7.4}$$
$$|\vec{u}|_{\Sigma^+} = |\vec{u}|_{\Sigma^-} \ \text{Continuity of (7.1) and of the pressure.} \tag{7.5}$$

Here n_Σ is the normal to Σ and Σ^+, Σ^-, indicate the value from above and below when the functions are discontinuous.

Problem (7.1)-(7.5) is well posed with the boundary conditions below acting on the normal component of $\vec{u}$:

$$\vec{u} \cdot n = \vec{u}_\infty \cdot n, \text{ on } \Gamma_\infty \tag{7.6}$$
$$\vec{u} \cdot n = 0 \text{ on } \Gamma. \tag{7.7}$$

In two dimensions (7.1) implies that there exists a scalar function $\psi(\vec{x})$ such that

$$\vec{u} = \nabla \times \psi = \left(\frac{\partial \psi}{\partial x_2}, -\frac{\partial \psi}{\partial x_1} \right). \tag{7.8}$$

Then (7.2) reduces to

$$\Delta \psi = 0 \text{ in } \Omega. \tag{7.9}$$

To find boundary conditions for ψ we use (7.6)-(7.7):

$$\nabla \psi \cdot t = \begin{cases} \vec{u}_\infty \cdot n, \text{ on } \Gamma_\infty \\ 0 \text{ on } \Gamma \end{cases} \tag{7.10}$$

where t is a tangent vector to the boundary. This equation can be integrated and give

$$\psi = u_{1\infty}x_2 - u_{2\infty}x_1 \text{ on } \Gamma_\infty, \tag{7.11}$$

$$\psi = \beta, \text{ constant on } \Gamma. \tag{7.12}$$

The constant β is not known but it can be found by imposing continuity of the flow at the trailing edge P:

$$\frac{\partial \psi}{\partial n} |_{P+} = -\frac{\partial \psi}{\partial n} |_{P-} \tag{7.13}$$

That is the Joukowski condition at trailing edge.

It can be shown that there is one and only one solution to (7.9)(7.11)(7.12)(7.13). Indeed the solution of (7.9)(7.11)(7.12) is linear in β and (7.13) is an equation to determine β. Mathematically it has been shown (see [8]) that it is also the only solution of (7.9)(7.11)(7.12) which belongs to $H^2(\Omega)$; when β does not satisfy (7.13), the solution has a singularity at the trailing edge and it is in $H^1(\Omega)$ but not in $H^2(\Omega)$.

7.1 Formulation of the aerodynamic problem

From a practical point of view, the easier way to solve the problem is to use the linearity in β; it also yields a description of the fluid problem analogous to the electromagnetic one.

Let ψ^0 and ψ^1 be the solution of

$$\begin{cases} \Delta\psi^0 = 0 \text{ in } \Omega \\ \psi^0 = u_{1\infty}x_2 - u_{2\infty}x_1 \text{ on } \Gamma_\infty \\ \psi^0 = 0 \text{ on } \Gamma, \end{cases} \tag{7.14}$$

$$\begin{cases} \Delta\psi^1 = 0 \text{ in } \Omega \\ \psi^1 = 0 \text{ on } \Gamma_\infty \\ \psi^1 = 1 \text{ on } \Gamma. \end{cases} \tag{7.15}$$

Then the solution to the problem is

$$\psi = \psi^0 + \beta\psi^1 \tag{7.16}$$

with β given by

$$\beta = -\frac{\frac{\partial \psi^0}{\partial n}|P+ + \frac{\partial \psi^0}{\partial n}|P-}{\frac{\partial \psi^1}{\partial n}|P+ + \frac{\partial \psi^1}{\partial n}|P-}. \tag{7.17}$$

It can be shown that the lift $\Lambda(\mathcal{S})$ of the airfoil (the vertical component of the force applied by the fluid on $\mathcal{S}$) is proportional to β:

$$\Lambda(\mathcal{S}) = \beta \rho \mid \vec{u}_\infty \mid \tag{7.18}$$

where ρ is the density of the fluid.
We see then, the analogy between the aerodynamical and the electromagnetic problem:

- On the computational domain Ω of the lift, we must solve two equations of the form $\Delta\psi = 0$, that is Helmholtz equations $\Delta\psi + k^2\psi = 0$ with $k = 0$.

- On the wing profile we have the Dirichlet conditions

$$\begin{aligned} \psi^0 &= 0, \\ \psi^1 &= 1, \end{aligned}$$

  as in the wave problem.

- At the "infinity boundary" Γ_∞ we have the Dirichlet conditions:

$$\begin{aligned} \psi^0 &= u_{1\infty}x_2 - u_{2\infty}x_1, \\ \psi^1 &= 0, \end{aligned}$$

  that is much simpler that the Sommerfeld radiation boundary condition.

A larger difference between electromagnetic and lift problems is as follows: The visibility is measured in a region Θ that is far from the control variable $\mathcal{S}$ (the airfoil). In the aerodynamic problem, the lift is calculated using the values of ψ^0 and ψ^1 at the trailing edge, and the geometry of this point could change in the course of the optimization problem. This is not the case here because the geometry of trailing edge is a design constraint which is given.

7.2 Discretization

Computationally (7.14)(7.15) can be solved as (5.1) with $k = 0$ and Dirichlet boundary conditions on $\Gamma \cup \Gamma_\infty$. Then the discretization, the computation of the lift and its gradient follow the lines of section (5).

Remark 1 *For the Joukowski condition one can in fact apply condition (7.13) by replacing P^+, P^- by the triangles which are on ∂S and have P as a vertex. See figure (7.1).*

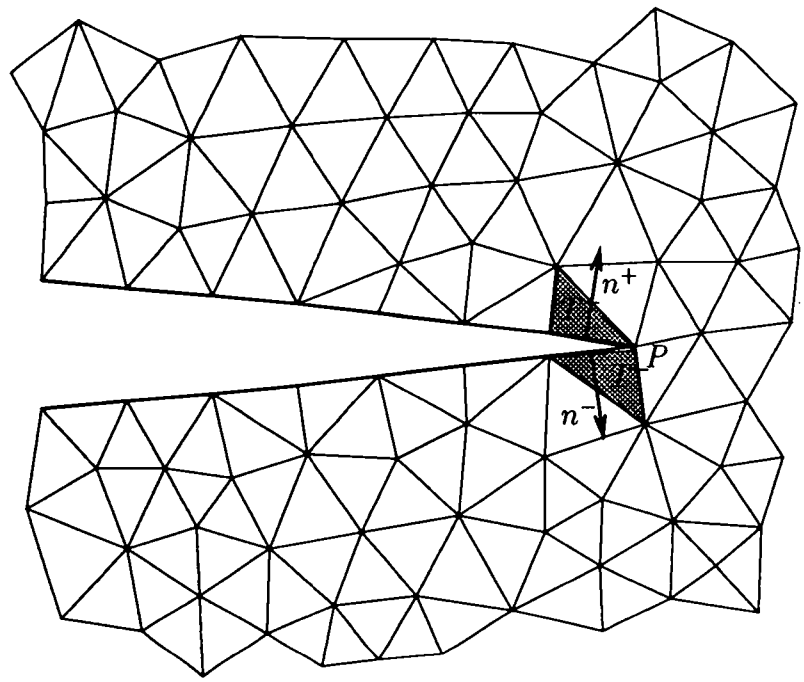

Figure 7.1: The trailing edge

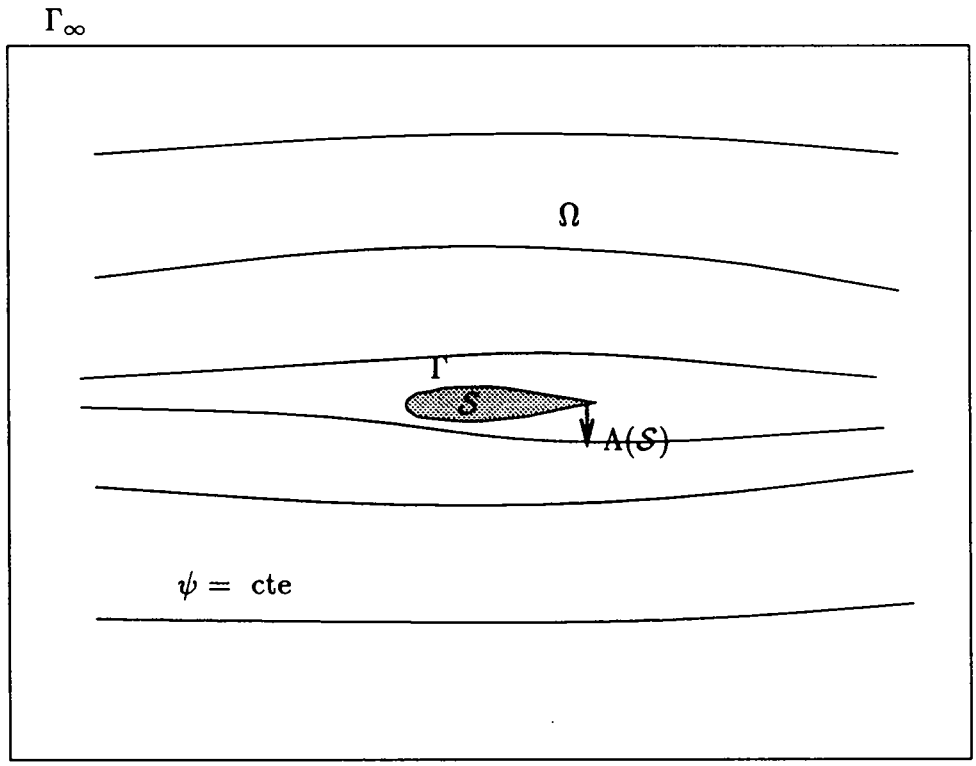

Figure 7.2: The stream close the airfoil

8 The Optimization Method

For our optimum design problem we use Herskovits' algorithm (see [9][10][11]). This is a strong and efficient method that is interesting in design problems because it generates a sequence of *feasible designs* converging to a Kuhn-Tucker (K-T) point of the problem. The fact that all designs of the sequence are feasible allows us to stop iterations when we think that the gain is sufficient. That is important for optimum design with expensive computing times.

8.1 General nonlinear optimization problem

Let us consider the constrained nonlinear optimization problem

$$\min_{x \in \Omega_{ad}} f(x) \tag{8.1}$$

where $\Omega_{ad} = \{x \in I\!R^n;\ g(x) \leq 0\}$ is the set of feasible designs. The functions $f : \Re^n \longrightarrow \Re$ and $g = (g_1, ..., g_m)^t : \Re^n \longrightarrow \Re^m$ are smooth. The expression $g(x) \leq 0$ means that $g_i(x) \leq 0,\ \forall\, i = 1, \cdots, m$.

8.2 The Kuhn-Tucker optimality conditions

A solution of this optimization problem satisfies the first order K-T optimality conditions below

$$\left\{ \begin{array}{rcl} \nabla f(x) + \sum_{i=1}^{m} \lambda_i \nabla g_i(x) & = & 0 \\ \lambda_i g_i(x) & = & 0,\ i = 1, \cdots, m \\ g_i(x) & \leq & 0,\ i = 1, \cdots, m \\ \lambda_i(x) & \geq & 0,\ i = 1, \cdots, m\ , \end{array} \right. \tag{8.2}$$

where x and λ are the primal and dual variable respectively. A solution (x^*, λ^*) of conditions (8.2) is named a Kuhn-Tucker pair of the system.

Definition 3 *A vector $d \in \Re^n$ is a descent direction of f at $x \in \Re^n$ if $\nabla f(x) \cdot d < 0$. See figure (8.1)*

Definition 4 *The vector $d \in \Re^n$ is a feasible direction of Ω_{ad} at $x \in \Omega_{ad}$, if for some $\theta > 0$ we have $x + td \in \Omega_{ad}$ for all $t \in [0, \theta]$. Then for any point x at the interior of Ω_{ad} all the directions are feasible. For x at the boundary, that is, if $g_i(x) = 0$ for some $i = 1, \cdots, m$, we have*

$$\nabla g_i(x) \cdot d < 0 \Longrightarrow \ d \text{ is feasible.} \tag{8.3}$$

This is the notion of feasibility that we use in our computations. See figure (8.2)

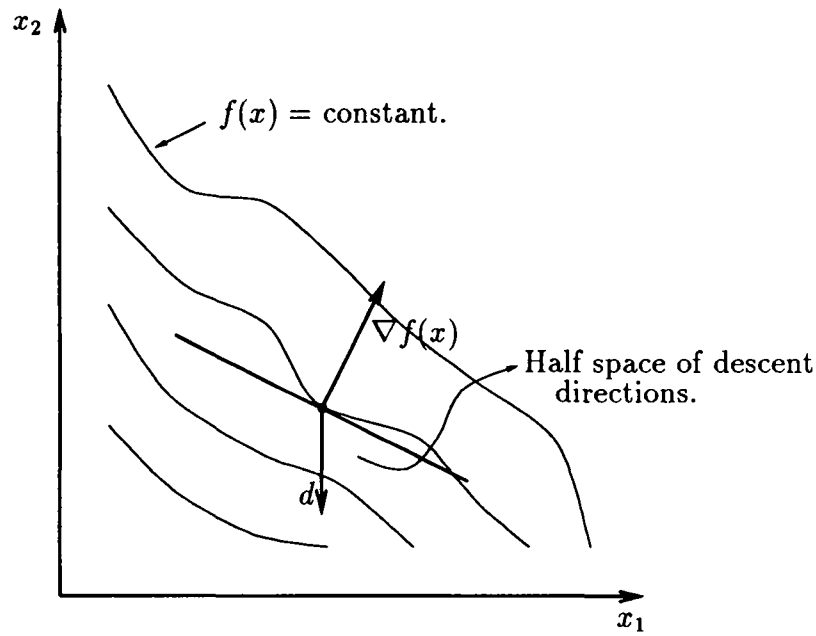

Figure 8.1: The descent directions

The algorithm we use, generates for a given initial interior point (feasible initial design) a sequence $\{x^k\}$ of feasible points (feasible designs) with decreasing values of the cost and converging to a K-T point x^* of the problem.
At each iteration a search direction d is defined, which is a *descent direction* of the objective and also a *feasible direction* of Ω_{ad}.

8.3 The Herskovits' algorithm

Let

$$L(x, \lambda) = f(x) + \lambda^t \cdot \mathbf{g}(x) \tag{8.4}$$

be the Lagrangian of (8.1) and

$$H(x, \lambda) = \nabla^2 f(x) + \sum_{i=1}^{m} \lambda_i \nabla^2 g_i(x) \tag{8.5}$$

its Hessian.
We define the matrices:

$$C(x) \;=\; [\nabla f(x)]^t \in M_{n\times 1}(\Re)$$

$$A(x) = \left[\frac{\partial g_j}{\partial x_i}(x)\right]_{i,j} \in M_{n\times m}(\Re)$$

and $G(x) \in M_m(\Re)$ the diagonal matrix, with $G_{ii}(x) = g_i(x)$.
Then the K-T first order optimality conditions can be written as

$$\begin{aligned} C(x) + A(x)\cdot\lambda &= 0, && (8.6)\\ G(x)\cdot\lambda &= 0, && (8.7)\\ g(x) &\leq 0, && (8.8)\\ \lambda &\geq 0. && (8.9) \end{aligned}$$

Being given x, λ, a Newton's iteration for the solution of (8.6)(8.7) gives x_0, λ_0, solution of the linear system:

$$\begin{bmatrix} B & A(x) \\ A^t(x)\cdot\Lambda & G(x) \end{bmatrix} \cdot \begin{bmatrix} x_0 - x \\ \lambda_0 - \lambda \end{bmatrix} = - \begin{bmatrix} C(x) + A(x)\cdot\lambda \\ G(x)\cdot\lambda \end{bmatrix} \qquad (8.10)$$

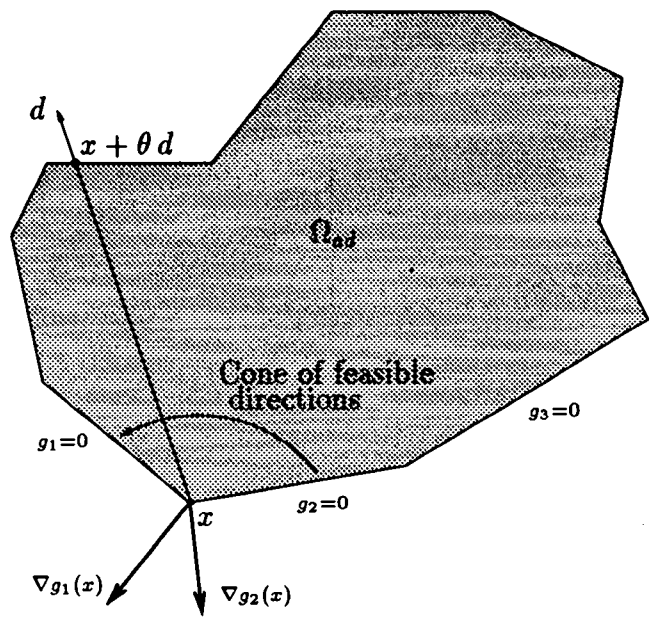

Figure 8.2: The feasible directions

Here $\Lambda \in M_n(\Re)$ is the diagonal matrix with $\Lambda_{ii} = \lambda_i$ and $B = H(x, \lambda)$, or a quasi-Newton approximation or the identity matrix. As a requirement for global convergence, B must be symmetric, positive definite.
Let us define the direction in the primal space $d_0 = x_0 - x$. Then we can write the last system as:

$$B \cdot d_0 + A(x) \cdot \lambda_0 = -C(x) \tag{8.11}$$
$$A^t(x) \cdot \Lambda \cdot d_0 + G(x) \cdot \lambda_0 = 0. \tag{8.12}$$

It is proved that d_0 is a descent direction of f. But d_0 is not always a feasible direction. Then we must introduce some modification to the Newton iteration so that, for a given interior pair x, λ, the new estimate is interior and the objective improved.
If x is on the boundary of Ω_{ad} then $g_i(x) = 0$ for some i. Then (8.12) implies that

$$\nabla g_i(x) \cdot d_0 = 0. \tag{8.13}$$

Thus d_0 is tangent to the active contraints, and may not be feasible.

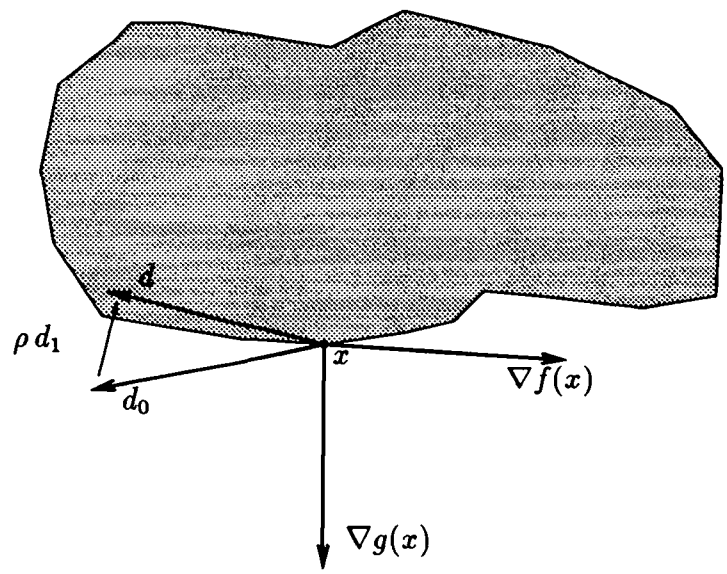

Figure 8.3: The deflected direction

To overcome this problem, we can change system (8.11)-(8.12) and compute $\overline{d}$, $\overline{\lambda}$ solution of the following linear system:

$$B \cdot \overline{d} + A(x) \cdot \overline{\lambda} = -C(x), \tag{8.14}$$
$$A^t(x) \cdot \Lambda \cdot \overline{d} + G(x) \cdot \overline{\lambda} = -\rho \Lambda \cdot \omega, \tag{8.15}$$

obtained by adding a negative vector in the right hand side of (8.12) with, $\rho \in \Re^+$, $\omega \in \Re^{+m}$.

In this case we have for an active contraint $g_i(x) = 0$

$$\nabla g_i(x) \cdot \overline{d} = -\rho\omega_i. \tag{8.16}$$

Thus $\overline{d}$ is a feasible direction.

The inclusion of a negative number in the right hand side of (8.12) produces the effect of deflecting d_0 towards the interior of the feasible region. See figure (8.3). This deflection, relative to the i-th constraint is proportional to $\rho\omega_i$.

Since the deflection of d_0 is proportional to ρ and d_0 is a descent direction, it is possible to establish bounds on ρ which ensure that $\overline{d}$ is also a descent direction of f at x. We obtain these bounds by imposing

$$\nabla f(x) \cdot \overline{d} \leq \alpha \nabla f(x) \cdot d_0, \tag{8.17}$$

and thus

$$\alpha \nabla f(x) \cdot d_0 < 0 \Longrightarrow \nabla f(x) \cdot \overline{d} < 0. \tag{8.18}$$

In general, the derivative of f in the direction of $\overline{d}$ will be smaller than in the direction of d_0. This is the price to pay to obtain feasible descent directions $\overline{d}$.

Finally once a feasible direction $\overline{d}$ is obtained, to determine a new primal point x, we make an inaccurate line search in the direction of $\overline{d}$, requiring feasibility and a sufficient decrease of the objective. To define a new positive λ we can choose different strategies.

9 The Absorbing Paint Problem

Until now, we have worked with an optimum design problem for a wing profile made of a perfectly conducting material. To reduce even more the radar visibility we can cover the wing with a coating paint layer absorbing radar waves. This paint layer is characterised by its composition (homogeneous or not), its electromagnetics properties and its local thickness.

9.1 The boundary condition for a coating paint

Using techniques of asymptotic expansion and homogeneisation we can describe the macroscopic effect of such paint layers, with a boundary condition on $\Gamma = \partial\mathcal{S}$. For a perfectly conducting material we have the Dirichlet homogeneous condition

$$w = 0 \text{ on } \partial\mathcal{S}. \tag{9.1}$$

In the case of a coating paint layer on the wing profile, the Leontowitch boundary condition is used (see [1][19]) :

$$\frac{\partial w}{\partial n} = -\alpha\, w \text{ on } \partial\mathcal{S}, \tag{9.2}$$

where α depends on:

- The geometry of $\partial\mathcal{S}$,
- electromagnetics properties of the coating paint,
- the thickness of the paint layer.

For an homogeneous material, see figure (9.1), we have the following first order approximation of α:

$$\alpha_\epsilon(x) = -\frac{\mu_1}{\mu_2}\frac{1}{\epsilon(x)}, \tag{9.3}$$

where μ_1 is the magnetic permeability of the medium, and μ_2 the permeability of the paint. The term ϵ is a function defined on $\partial\mathcal{S}$, such that $\epsilon(\vec{x})$ is the thickness (positive) of paint in the direction of unit external normal vector, $\vec{n}$.

Let w_ϵ the electromagnetic total wave, be decomposed in $w_\epsilon = z + y_\epsilon$, where $z(\vec{x}) = e^{i\vec{k}\cdot\vec{x}}$ is the plane incident wave and y_ϵ the stationary wave diffracted by the obstacle. On $\partial\mathcal{S}$, we have then

$$\frac{\partial w_\epsilon}{\partial n} = -\alpha\, w_\epsilon \Longrightarrow \frac{\partial y_\epsilon}{\partial n} = -\alpha_\epsilon\, y_\epsilon - \left(\frac{\partial z}{\partial n} + \alpha_\epsilon z\right) \text{ on } \partial\mathcal{S}. \tag{9.4}$$

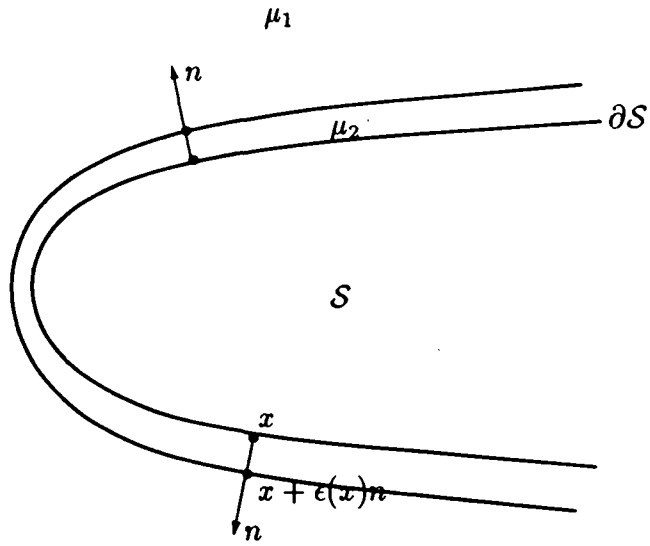

Figure 9.1: The homogeneous paint layer

Then the optimisation problem we solve here is:

Problem:

$$\text{Minimise } j(\epsilon) = J(y_\epsilon) = \int_\Theta |\, y_\epsilon \,|^2 \, d\theta \tag{9.5}$$

where y_ϵ is solution of

$$\begin{cases} \Delta y_\epsilon + k^2 y_\epsilon = 0 & \text{in } \Omega \\ \dfrac{\partial y_\epsilon}{\partial n} = -\alpha_\epsilon y_\epsilon - \left(\frac{\partial z}{\partial n} + \alpha_\epsilon z\right) & \text{on } \partial S \\ \dfrac{\partial y_\epsilon}{\partial n} = \mathcal{M} y_\epsilon & \text{on } \partial D. \end{cases} \tag{9.6}$$

9.2 Variational formulation and approximation

We use the variational formulation of the problem for its finite element method approximation. First we replace (9.6) by

$$\int_\Omega [\nabla y_\epsilon \cdot \nabla \phi - k^2 y_\epsilon \cdot \phi]\, d\Omega + \int_{\partial D} \mathcal{M} y_\epsilon \cdot \phi + \int_\Gamma \alpha_\epsilon y_\epsilon \phi = \int_\Gamma \left(-\frac{\partial z}{\partial n} - \alpha_\epsilon z\right) \cdot \phi, \quad \forall \phi \in H^1(\Omega). \tag{9.7}$$

We take a mesh Ω_h of the domain Ω, and a space $H_h^1(\Omega_h)$ of piecewise polynomial functions of degree 1 in Ω_h. The approximation of y_ϵ is given by $y_{h\epsilon} \in H_h^1(\Omega_h)$ such that

$$\int_{\Omega_h} [\nabla y_{h\epsilon} \cdot \nabla \phi_h - k^2 y_{h\epsilon} \cdot \phi_h] \, d\Omega_h + \int_{\partial D_h} \mathcal{M}_h y_{h\epsilon} \cdot \phi_h + \int_{\Gamma_h} \alpha y_{h\epsilon} \phi_h = - \int_{\Gamma_h} \left(\frac{\partial z}{\partial n} + \alpha_\epsilon z \right) \cdot \phi_h \tag{9.8}$$

for all discrete test functions $\phi_h \in H_h^1(\Omega_h)$. The term $\mathcal{M}_h$ is a discrete approximation on ∂D_h of $\mathcal{M}$.

Let n_h be the dimension of $H_h^1(\Omega_h)$, and $\{q_{jh}\}$ its finite element basis, associated to the mesh. The approximate solution being of the form

$$y_{h\epsilon} = \sum_{j=1}^{n_h} y_\epsilon^j \cdot q_{jh} \tag{9.9}$$

we get the finite dimensional linear system of grid equations

$$\int_{\Omega_h} [\nabla y_{h\epsilon} \cdot \nabla q_{jh} - k^2 y_{h\epsilon} \cdot q_{jh}] \, d\Omega_h + \int_{\partial D_h} \mathcal{M}_h y_{h\epsilon} \cdot q_{jh} + \int_{\Gamma_h} \alpha_\epsilon y_{h\epsilon} q_{jh} = - \int_{\Gamma_h} \left(\frac{\partial z}{\partial n} + \alpha_\epsilon z \right) \cdot q_{jh} \tag{9.10}$$

for all $j = 1, \ldots, n_h$,

This system can be written as

$$A_{ij} y_\epsilon^j = B_i \,, \quad i = 1, \ldots, n_h. \tag{9.11}$$

where $A = \left[A_{ij}^\epsilon\right] \in M_{n_h}(C)$, $B^\epsilon = [B_i^\epsilon] \in M_{n_h \times 1}(C)$, $Y_\epsilon \in M_{n_h \times 1}(C)$,

$$\begin{aligned} A_{ij}^\epsilon &= \int_{\Omega_h} [\nabla q_{ih} \cdot \nabla q_{jh} - k^2 q_{ih} \cdot q_{jh}] \, d\Omega_h + \int_{\partial D_h} \mathcal{M}_h q_{ih} \cdot q_{jh} + \int_{\Gamma_h} \alpha_\epsilon q_{ih} q_{jh} \\ B_i^\epsilon &= - \int_{\Gamma_h} \left(\frac{\partial z}{\partial n} + \alpha_\epsilon z \right) \cdot q_{ih} \\ Y_\epsilon &= \left[y_\epsilon^i\right]. \end{aligned}$$

At the discrete level, the paint thickness ϵ is given by some parameters $\sigma = (\sigma_1, \ldots, \sigma_K)$ which describe ϵ by

$$\epsilon(\sigma) = \sigma_1 \epsilon_1(x) + \ldots + \sigma_K \epsilon_K(x) \tag{9.12}$$

where ϵ_k, $k = 1, \ldots, K$ are fixed polynomial piecewise linear functions on Γ_h or splines.

The cost function depends on the values of these parameters, that is, $j_h = j_h(\sigma_1, \ldots, \sigma_K)$. If the radius R of D is large enough we have that $\mid y_\epsilon(R, \cdot) \mid$ is a good approximation of the radiation diagram, and then we consider that the cost function is

$$\begin{aligned} j_h(\sigma_1, \ldots, \sigma_K) &\stackrel{def}{=} \frac{1}{2}\int_\Theta \mid y_{h\epsilon} \mid^2 d\theta_h \\ &= \frac{1}{2}\int_\Theta \sum_{i,j=1}^{n_h} y_\epsilon^i \cdot \overline{y_\epsilon^j}\, q_{ih} \cdot q_{jh}\, d\theta \\ &= \frac{1}{2}\overline{Y_\epsilon}^t \cdot C \cdot Y_\epsilon \end{aligned}$$

where

$$C = [C_{ij}] = \left[\int_\Theta q_{ih} \cdot q_{jh}\, d\theta\right] \in M_{n_h}(\Re). \tag{9.13}$$

This term is a classical linear quadratic optimal control problem [12].

9.3 Computation of the discrete gradient

We define the Lagrangian

$$\mathcal{L} : \Re^K \times M_{n_h \times 1}(C) \times M_{n_h \times 1}(C) \longrightarrow \Re \tag{9.14}$$

$$\mathcal{L}(\sigma, Y, P) = \frac{1}{2}\overline{Y} \cdot C \cdot Y + Re\left\{P^t \cdot \left[A^{\epsilon(\sigma)} \cdot Y - B^{\epsilon(\sigma)}\right]\right\}. \tag{9.15}$$

The Kuhn-Tucker optimality conditions give:

9.3.1 i) Discrete state equation.

$Y_{\epsilon(\sigma)}$ verifies

$$\frac{D\mathcal{L}}{DP}\left(\sigma, Y_{\epsilon(\sigma)}, P\right) = 0 \Longleftrightarrow A^{\epsilon(\sigma)} \cdot Y_{\epsilon(\sigma)} = B^{\epsilon(\sigma)}. \tag{9.16}$$

9.3.2 ii) Discrete adjoint equation.

Let $P^{\epsilon(\sigma)}$ be, by definition, the adjoint state, solution of the adjoint equation

$$\frac{D\mathcal{L}}{DY}\left(\sigma, Y_{\epsilon(\sigma)}, P_{\epsilon(\sigma)}\right) = 0 \Longleftrightarrow A^{\epsilon(\sigma)^t} \cdot P_{\epsilon(\sigma)} = C \cdot \overline{Y}_{\epsilon(\sigma)}. \tag{9.17}$$

9.3.3 iii) Gradient of the cost function.

We have that

$$j_h(\sigma) = \mathcal{L}\left(\sigma, Y_{\epsilon(\sigma)}, P_{\epsilon(\sigma)}\right) \tag{9.18}$$

and then $\forall\, k \in \{1, \ldots, K\}$

$$\begin{aligned}
\frac{D\, j_h}{D\, \sigma_k} &= \frac{D\, \mathcal{L}}{D\, \sigma_k}\left(\sigma, Y_{\epsilon(\sigma)}, P_{\epsilon(\sigma)}\right) + \frac{D\, \mathcal{L}}{D\, W}\left(\sigma, Y_{\epsilon(\sigma)}, P_{\epsilon(\sigma)}\right) \cdot \frac{D\, W}{D\, \sigma_k} + \frac{D\, \mathcal{L}}{D\, P}\left(\sigma, Y_{\epsilon(\sigma)}, P_{\epsilon(\sigma)}\right) \cdot \frac{D\, P}{D\, \sigma_k} \\
&= \frac{D\, \mathcal{L}}{D\, \sigma_k}\left(\sigma, Y_{\epsilon(\sigma)}, P_{\epsilon(\sigma)}\right) \\
&= Re\left\{ P^t_{\epsilon(\sigma)} \cdot \left[\frac{D\, A^{\epsilon(\sigma)}}{D\, \sigma_k} \cdot Y_{\epsilon(\sigma)} - \frac{D\, B^{\epsilon(\sigma)}}{D\, \sigma_k} \right] \right\}.
\end{aligned}$$

The optimisation problem can now proceed as before.

10 Numerical exemples

We consider an airfoil NACA0012 and we apply to it the optimisation techniques described above both, for geometric optimisation and paint layer thickness optimisation.

10.1 Geometrical optimisation

We consider that on the wing profile incides a plane wave, z, with an angle of 15° and with a wavelength of 1/5 of the length of the airfoil:

$$\begin{aligned} \alpha &= 15\pi/180, \\ k &= 2\pi/5, \\ \vec{k} &= k\,(\cos\alpha, \sin\alpha)\,, \\ z(\vec{x}) &= e^{i\vec{k}\vec{x}}. \end{aligned}$$

We want to minimize the radiation in a sector close to the incident wave. We have taken the sector corresponding to $[180°, 210°]$. On figure (10.2) we see the diffracted wave close to the airfoil NACA0012. The triangulation has 12,000 vertices, that is approximatly 15 points per wavelength.

10.1.1 Weakly constrained problem

On the wing profile we consider the constraint that its points cannot differ more than 15% of the initial NACA0012. The final profile and the diffracted wave close to it are shown on figure (10.3). It is obtained after 12 iterations and the number of control points is 60. The cost function has been decreased by 500%. See figure (10.9).

The comparison between the radiation diagrams of the NACA0012 and the optimised profile is shown on figure (10.5). The initial radiation diagram is the curve in bold and the final is drawn with a thin line.

We see the gain in the reduction of the radiation diagram around 195°, but the wing profile is not good aerodynamically.

10.1.2 Strongly constrained problem

We keep the contraints of the *weakly constrained problem* and add two others constraints.

- First, the curvature of the wing profile at control points is bounded.
- Second, we impose an aerodynamic constraint on the lift coefficient, which must be greater than 0, for an angle of incidence of 15°.

On figure (10.4) we see the obtained wing profile and the diffracted wave. The comparison between the final and initial radiation diagrams is shown on figure (10.6): 23 iterations reduce the cost fuction by 20%. See figure (10.10).

The stream function around the NACA0012 is shown on figure (10.7). The stream function around the optimised airfoil is shown on figure (10.8).

Clearly, the gain is not as large as in the weakly constrained problem, but this airfoil is physically feasible.

10.2 Paint thickness optimisation

Here we consider the wing profile NACA0012 with an initial thin uniform distribution of paint, and we optimise the paint thickness in every point of the wing profile to minimise the visibility. In this test we consider an incident wave with an angle of 45° and with $k = 30$.

We want to minimise the visibility in a sector near 225°.

On figure (10.11) we see the diffracted wave close to the airfoil for the initial constant paint layer. Figure (10.12) shows the same thing for the optimised distribution of paint.

The initial and final paint distribution are showed on figures (10.13)(10.14). The paint thickness has been scaled up for graphical reasons. On figure (10.13) the thickness is closed to zero and and we see mainly the geometry of NACA0012. On figure (10.15) we see that 9 iterations reduce the cost by 40%.

The oscillations of paint thickness in (10.14) points to the use of coating non-homogeneous materials to reduce the visibility. See figure (10.1). That will be a next step in our work.

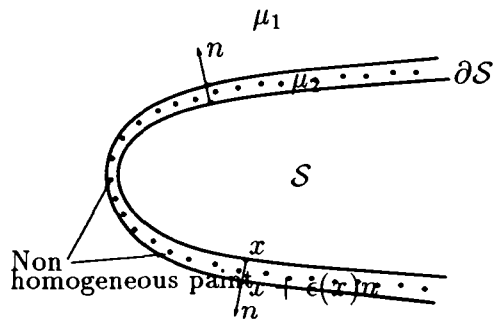

Figure 10.1: Non homogeneous paint layer

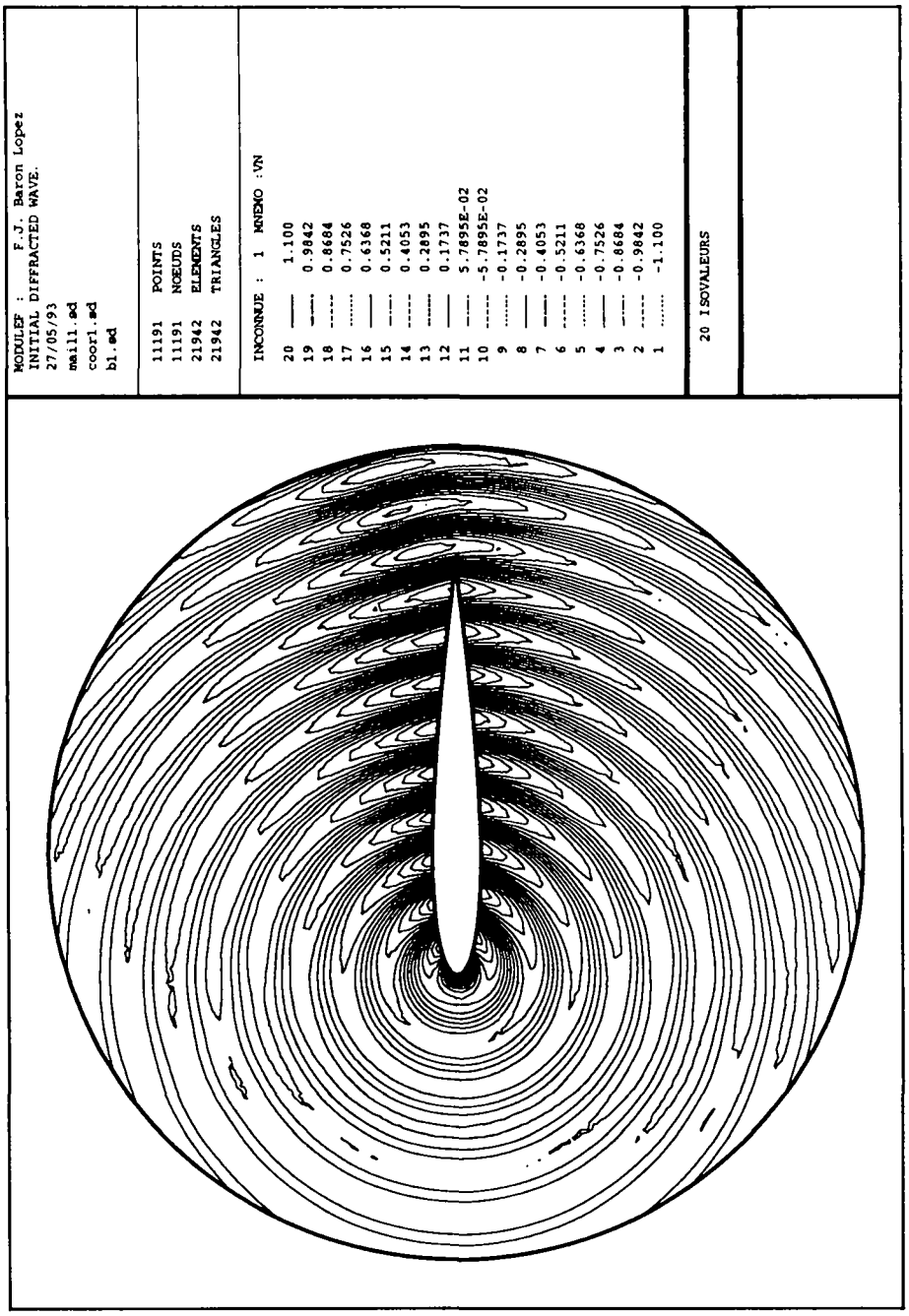

Figure 10.2: Initial diffracted wave

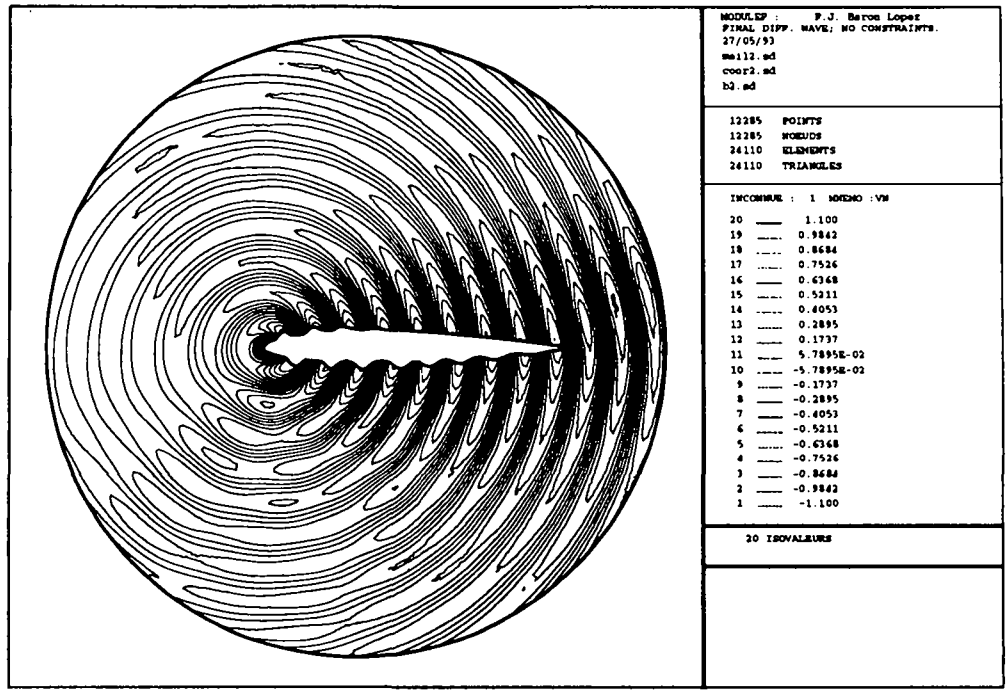

Figure 10.3: Final diffracted wave. Weakly constrained

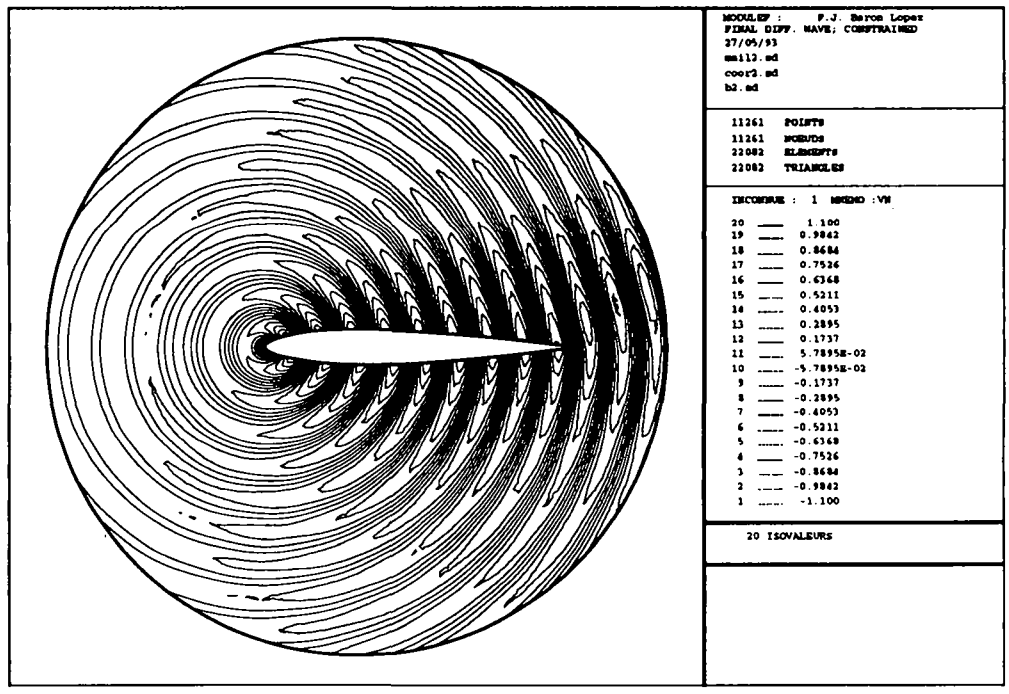

Figure 10.4: Final diffracted wave. Strongly constrained

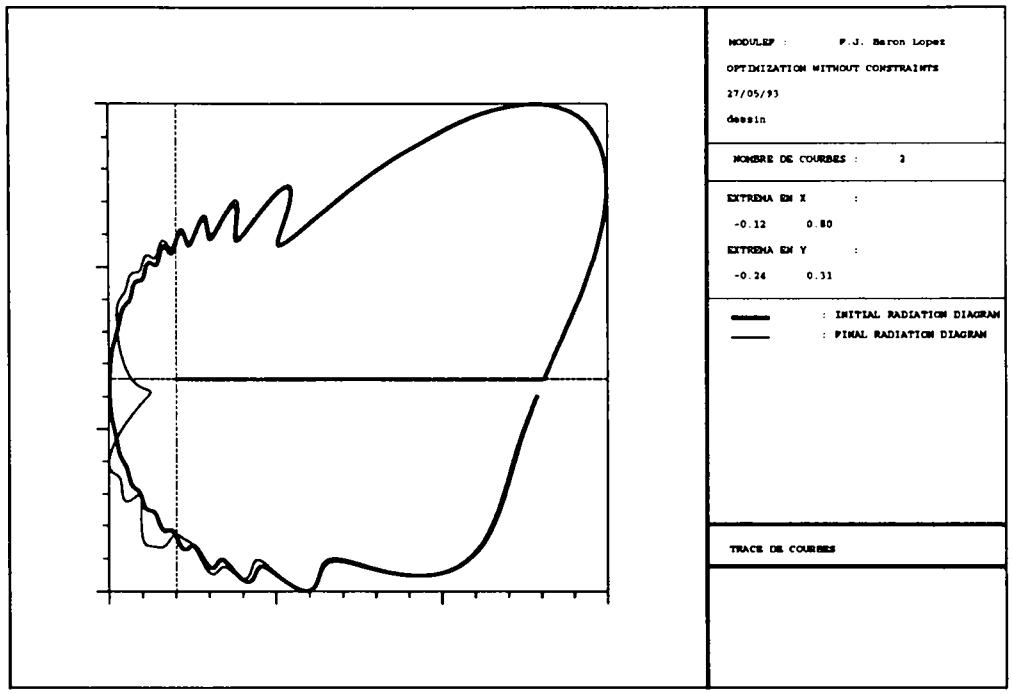

Figure 10.5: Initial and final SER. Weakly constrained

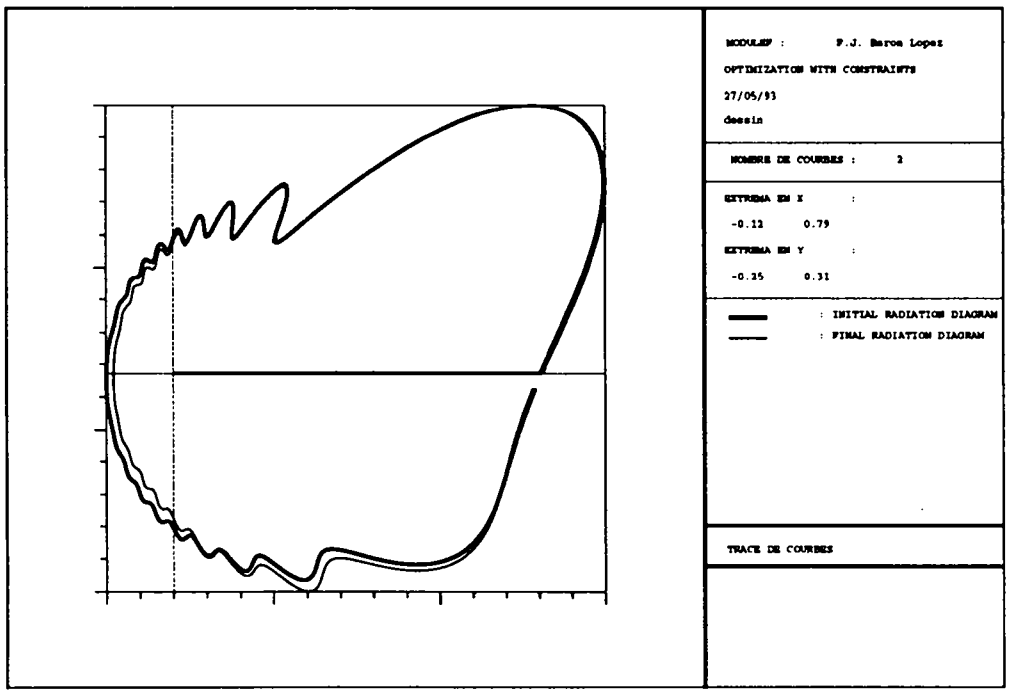

Figure 10.6: Initial and final SER. Strongly constrained

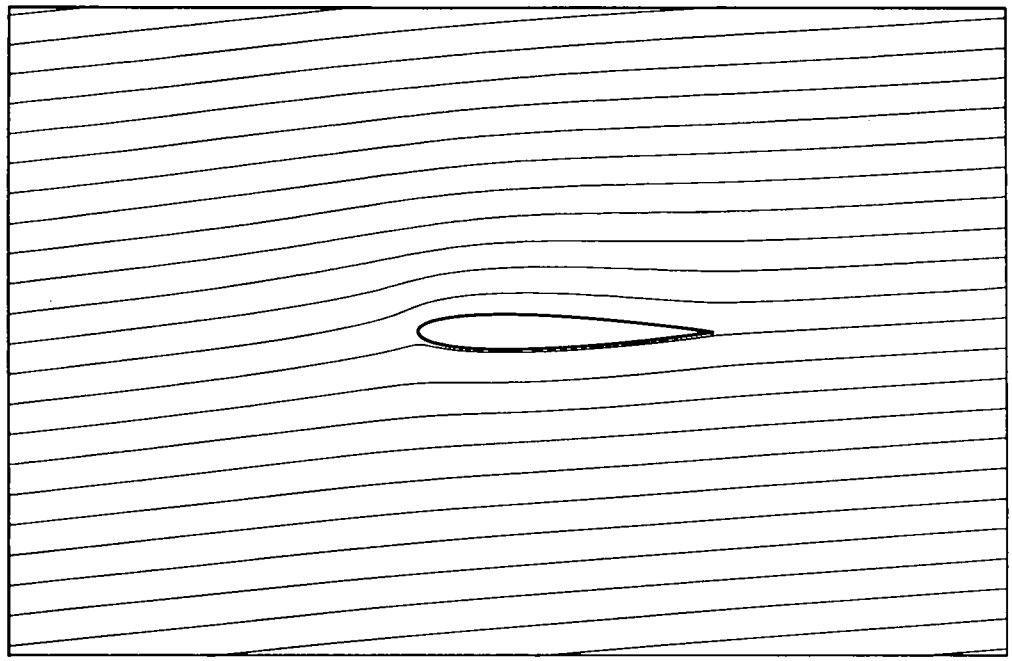

Figure 10.7: The stream around initial airfoil.

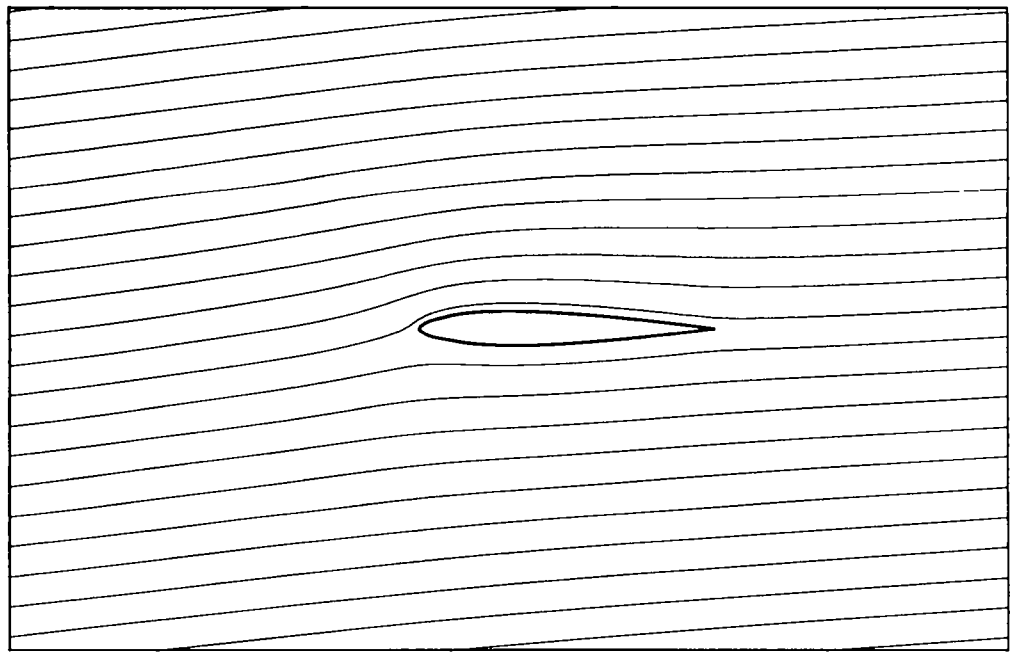

Figure 10.8: The stream for optimised airfoil. Strongly constrained

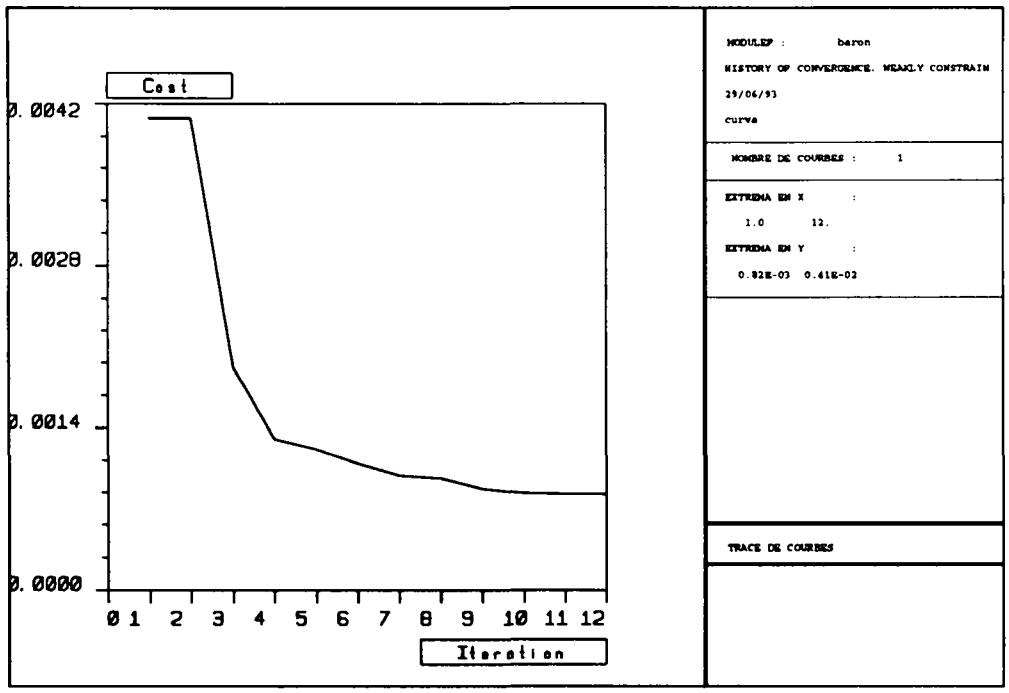

Figure 10.9: Convergency of the weakly constrained problem

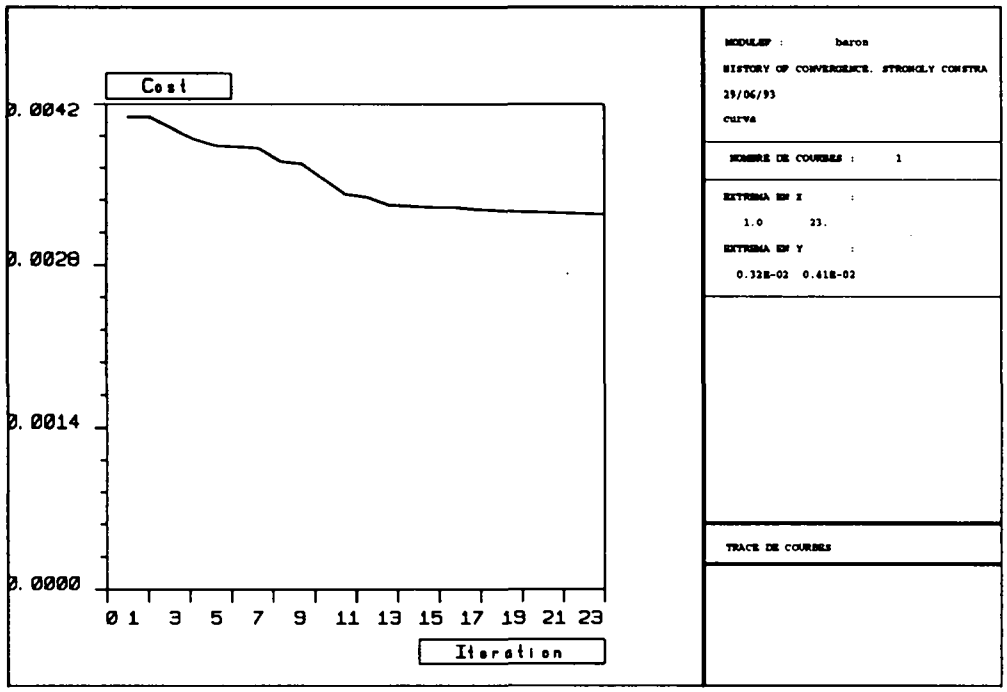

Figure 10.10: Convergency of the strongly constrained problem

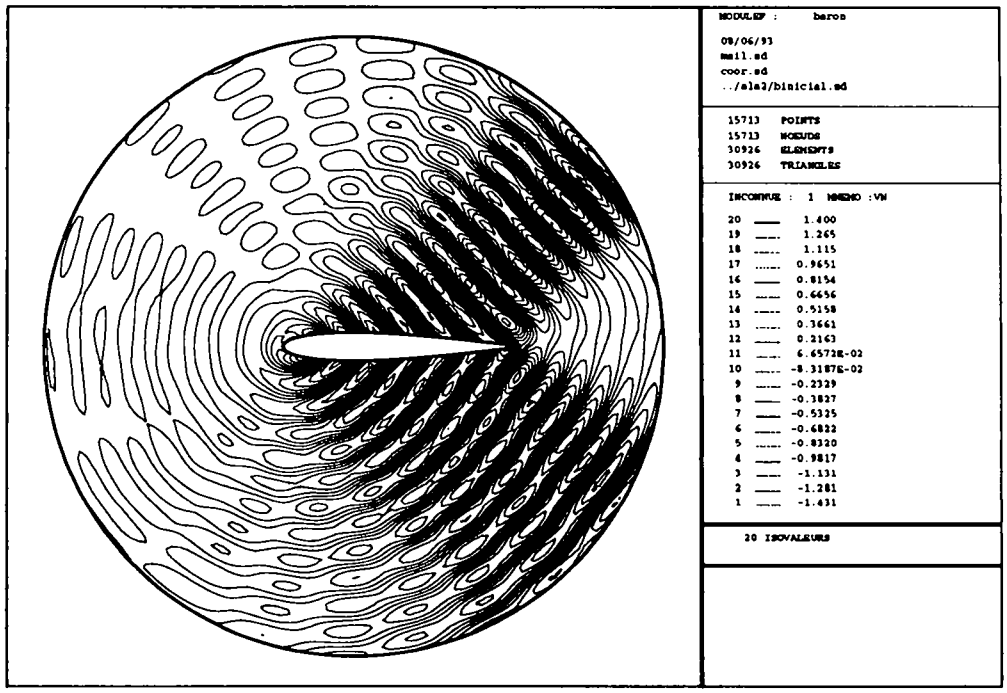

Figure 10.11: Initial diffracted wave.

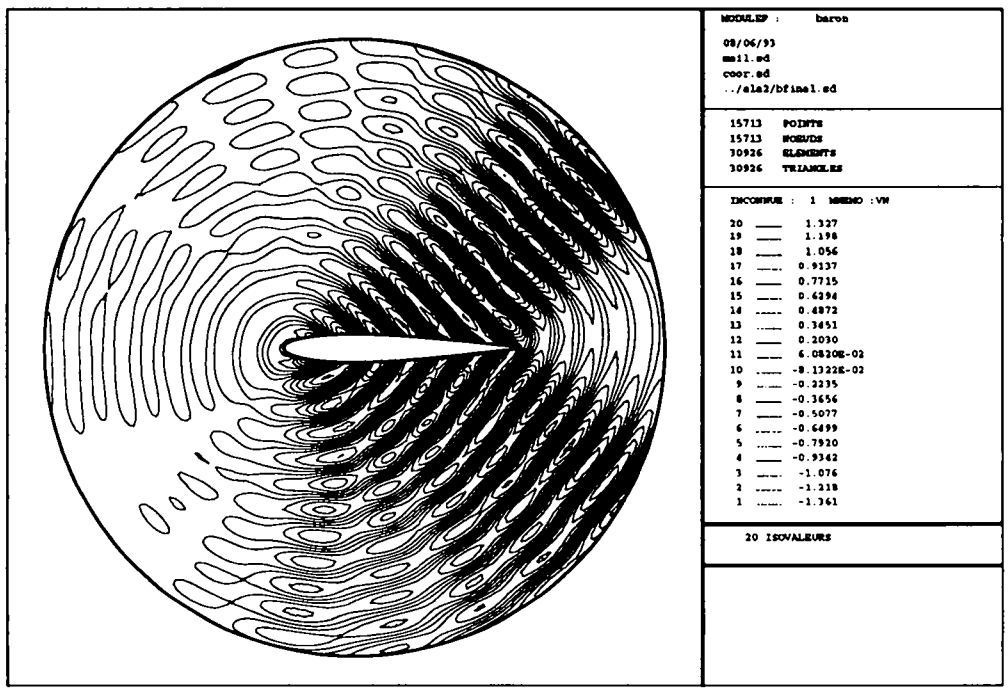

Figure 10.12: Final diffracted wave

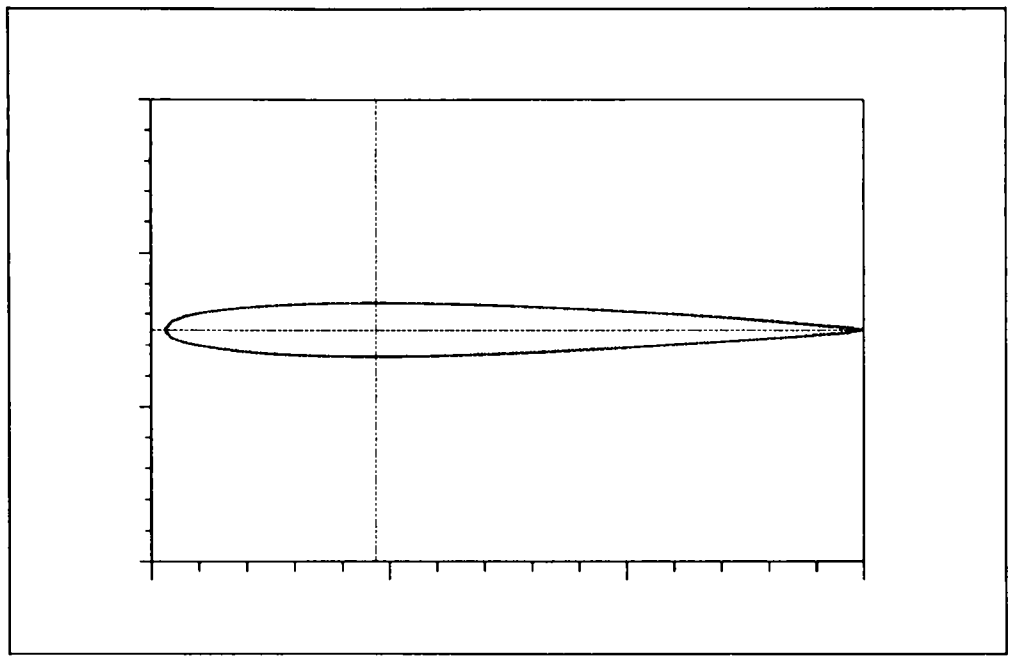

Figure 10.13: The initial paint layer.

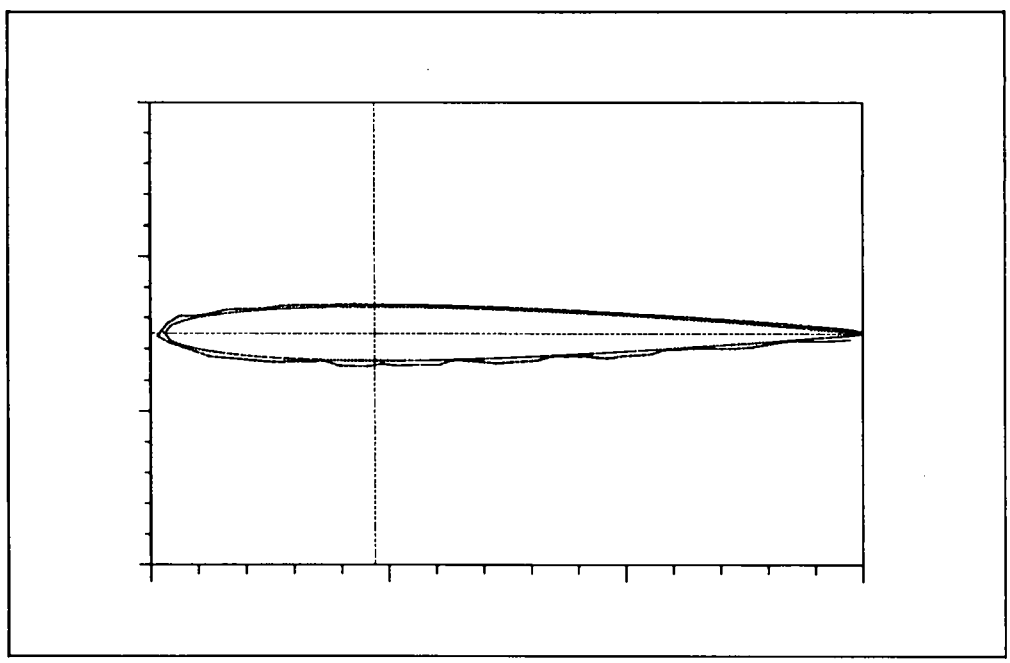

Figure 10.14: The optimised paint layer.

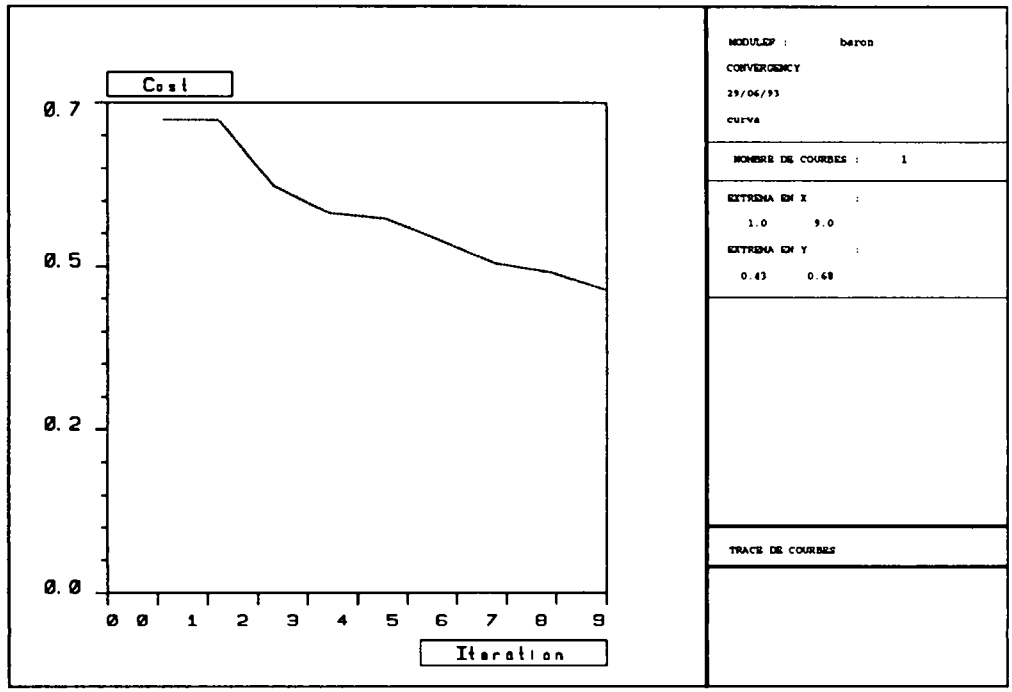

Figure 10.15: Convergency of the coating paint problem

11 Conclusion

Here we have not solved the global optimum design problem of a wing profile. Rather we show a method that we think is good to approach the problem of optimum design of a shape and, in particular, of an airfoil shape.

In a real problem of optimum design we must minimise some criteria. We can not change arbitrarily the conception variables to achieve the minimisation. Certaint constraints must be satisfied and maybe they are not of the same nature that the criteria to minimise, and not easy to compute. For example, in the problem that we consider here, we must reduce the radar visibility of a wing profile considering a aerodynamic constraints on lift. A change of the wing shape can reduce its radar visibility but we can loose the aerodynamical perfomances more that we can accept and viceversa. Thus it is necessary to relate the two disciplines, aerodynamic and electromagnetic, in the optimisation process.

In a real 3D optimisation problem of an airfoil we must also consider elastic criterias. For example, the flow around the wing produces elastic deformation of the wing, and this deformation changes this flow. Also, the deformation produces a stress field on the wing that must not be large. Then the stress field must be considered as a constraint on the design.

Another source of constraints is as follows. All the magnitudes above mentioned must be computed using mathematical models that are approximations of the physical reality. These models are good approximations if the shape (wing) to optimise verifies some geometrical constraints that allow us to say that the shape is, in fact, a wing profile, and that the computed magnitudes are meaningful. For example, a wing profile cannot have strong oscillations on its geometry (figure (10.3)), not only by physical reasons but also because a simple mathematical model (potential flow) cannot be used for the flow computation around it, and we should use more complicated models.

Thus the choice of the model for the computation of the different criterias (aerodynamical, electrodinamical, ...) implies a set of geometrical constraints to ensure the physical meaning of the computations.

In this work we use a method that has shown to be robust and efficient for this first application in multidisciplinary design. It is based in the nonlinear constrained optimisation algorithm of Herskovits. This algorithms allow us to generate a sequence of feasible designs verifiying the imposed constraints. The sequence has decreasing values of the cost and converges to a stationary point of the problem. The strength of the method suggests us that should be useful for treating more complex design problems.

List of Figures

References

[1] Y. ACHDOU, *Contributions à l'étude numérique des réseaux en électromagnetisme et de la couche limite en mécanique des fluides.* thesis, Paris 6, 1990.

[2] J.A. BELLO JIMÉNEZ, E. FERNÁNDEZ CARA, 'Control geométrico, diferenciación respecto de dominios y aplicaciones (Navier-Stokes)'. *Proceedings of "Jornadas hispano-francesas sobre control de sistemas distribuidos", Grupo de Análisis Matemático Aplicado de la Universidad de Málaga*, no. 3, (October 1.990).

[3] J.A. BELLO JIMÉNEZ, *Diferenciación respecto de dominios, regularidad L^r para los problemas de Stokes y Navier-Stokes y aplicaciones en control geométrico.* thesis, Universidad de Sevilla, 1992.

[4] A. BESPALOV, Y. KUZNETSOV, O. PIRONNEAU, M.-G. VALLET, 'Fictitious domains with separable preconditioners versus unstructured adapted meshes'. *Rapport de recherche INRIA, Rocquencourt*, no. 1614 (April 1992).

[5] A. BESPALOV, 'Application of fictitious domain method to the solution of the Helmholtz equation in unbounded domain'. *Rapport de recherche INRIA, Rocquencourt*, no. 1797, (November 1992).

[6] J. CEA, 'Conception optimale ou identification de formes: calcul rapide de la dérivée directionnelle de la fonction coût'. University of Nice, (1984).

[7] J.C. GILBERT, G. LE VEY, J. MASSE, 'La différentiation automatique de fonctions representées par des programmes'. *Rapport de recherche INRIA, Rocquencourt*, no. 1557, (November 1991).

[8] P. GRISVARD *Elliptic problems in non-smooth domains.* Pitman, 1985.

[9] J. HERSKOVITS, 'A two-stage feasible direction algorithm including variable metric techniques for nonlinear optimization problems'. *Rapport de recherche INRIA, Rocquencourt*, no. 118 (February 1982).

[10] J. HERSKOVITS, 'A two-stage feasible directions algorithm for nonlinear constrained optimization'. *Mathematical Programming*, **36**, pp. 19-38, (1986).

[11] J. HERSKOVITS, J. ASQUIER, 'Quasi-Newton interior points algorithms for nonlinear constrained optimisation'. *DGOR-Proceedings of Operations Research 1990*, Vienna, (August 1990).

[12] J.-L. LIONS, *Contrôle optimal des systêmes gouvernés par des equations aux derivées partielles.* Dunod, Paris, 1968.

[13] A. MARROCCO, 'Simulations numériques dans la fabrication des circuits a semiconducteurs (process modelling)'. *Rapport de recherche INRIA, Rocquencourt*, no. 305 (May 1984).

[14] O. PIRONNEAU, *Optimal shape design for elliptic systems*. Springer Series in Computational Physics, New York, 1984.

[15] O. PIRONNEAU, A. VOSSINIS, 'Comparision of some optimization algorithms for optimum shape design in aerodynamics'. *Rapport de recherche INRIA, Rocquencourt*, no. 1392, (February 1991).

[16] E. SANCHEZ PALENCIA, *Non-homogeneous media and vibration theory*. Lecture Notes in Physics, Springer-Verlag, Heidelberg, 1980.

[17] A. VOSSINIS, *Optimisation de forme d'aile d'avion*. Thesis, Paris 6, April 1993.

[18] A. ZEBIC, 'Equation de Helmholtz: étude numérique de quelques préconditionnements pour la méthode GMRES'. *Rapport de recherche INRIA, Rocquencourt*, no. 1802, (December 1991).

[19] A. ZEBIC, 'Applications de l'équation de Helmholtz à la diffraction d'ondes pour des obstacles revêtus de couches minces de matériaux électromagnétiques' *Rapport de recherche INRIA, Rocquencourt*, no. to appear.

Unité de Recherche INRIA Rocquencourt
Domaine de Voluceau - Rocquencourt - B.P. 105 - 78153 LE CHESNAY Cedex (France)

Unité de Recherche INRIA Lorraine Technopôle de Nancy-Brabois - Campus Scientifique
615, rue du Jardin Botanique - B.P. 101 - 54602 VILLERS LES NANCY Cedex (France)
Unité de Recherche INRIA Rennes IRISA, Campus Universitaire de Beaulieu 35042 RENNES Cedex (France)
Unité de Recherche INRIA Rhône-Alpes 46, avenue Félix Viallet - 38031 GRENOBLE Cedex (France)
Unité de Recherche INRIA Sophia Antipolis 2004, route des Lucioles - B.P. 93 - 06902 SOPHIA ANTIPOLIS Cedex (France)

EDITEUR
INRIA - Domaine de Voluceau - Rocquencourt - B.P. 105 - 78153 LE CHESNAY Cedex (France)

ISSN 0249 - 6399